EVALUATION OF PERMANENT DEFORMATION AND FATIGUE CRACKING RESISTANCE CHARACTERISTICS OF RECYCLED ASPHALT PAVEMENT BINDER

FINAL RESEARCH REPORT

URI-CVET-98-1

Prepared for

The Rhode Island Department of Transportation

By

K. Wayne Lee, Principal Investigator
Arun Shukla, Co-Principal Investigator
Sanjiv Venkatram, Graduate Research Assistant
Nikone Soupharath, Undergraduate Research Assistant

Department of Civil & Environmental Engineering
Department of Mechanical Engineering
College of Engineering
THE UNIVERSITY OF RHODE ISLAND

July, 1998

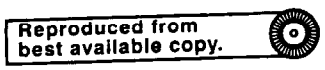

Technical Report Documentation Page

1. Report No.	2. Government Accession No.	3. Recipient's Catalog No.
4. Title and Subtitle Evaluation of Cracking and Pavement Deformation Resistance Characteristics of Recycled Asphalt Pavement Binder		5. Report Date August 25, 1998 6. Performing Organization Code
7. Author (s) K. Wayne Lee,Arun Shukla, Sanjiv Venkatram, and Nikone Soupharath		8. Performing Organization Report No. URI-CVET-98-1
9. Performing Organization Name and Address Department of Civil and Environmental Engineering University of Rhode Island Kingston, RI 02881		10. Work Unit No. (TRAIS) 11. Contract or Grant No. SPR-224-2235 13. Type of Report and Period Covered
12. Sponsoring Agency Name and Address Research and Technology Development Rhode Island Department of Transportation Providence, RI 02903		14. Sponsoring Agency Code
15. Supplementary Notes		

16. Abstract

This report presents experimental investigation results to evaluate the permanent deformation and cracking resisting characteristics of recycled asphalt pavement (RAP) binder. In the present study, two base asphalt binders (AC-10 and AC-20) typically used in Rhode Island were blended with different amounts of RAP binders obtained from two sources, i.e., 0, 10, 20, 30, 40, 50, 75, and 100%. The Dynamic Shear Rheometer (DSR) was used to evaluate the blended asphalt binders at high temperatures, i.e., 52, 58, 64, 70, and 76°C and intermediate temperatures, i.e., 19, 22, 25, 28, and 31°C. A good linear relationship between the log-log of the dynamic shear and the amount of RAP binder was obtained from this study. It was found that the addition of RAP binder generally increases the resistance against permanent deformation.

For the quasi-static loading experiments, it was observed that the compressive strength and the stiffness were increased and the ductilities were reduced as the amount of RAP increased. The fracture toughness was evaluated at different loading rates in order to study the rate dependency of the binder. It was observed that the fracture toughness values are increased gradually and then stabilized for the rates of loading over 152.4 mm per minute. Subsequently, a series of experiments was conducted at this rate to evaluate the fracture toughness of asphalt binder with different amounts of RAP, both at room and at low temperatures, i.e., 22 and 0°C, respectively. Results from the room temperature experiments indicated an increasing trend of fracture toughness as a function of RAP content. A brittle fast fracture occurred at low temperature and interestingly, RAP had no significant effect on the performance of the base asphalt binder. The dynamic response of RAP was evaluated using the Split Hopkinson Pressure Bar apparatus. The dynamic flow stress was found to increase with RAP content much like the variation in compressive strength under quasi-static conditions. The dynamic flow stress was not affected by incorporating RAP at low temperature.

17. Key Words	18. Distribution Statement
Recycled asphalt pavement, asphalt mixture, permanent deformation, fatigue cracking, rutting, low-temperature cracking, Superpave, rheological properties, dynamic shear rheometer, mechanical properties, compressive strength, fracture toughness, Split Hopkinson Pressure Bar.	

19. Security Classif. (of this report)	20. Security Classif. (of this page)	21. No. of Pages	22. Price
		89	

Form DOT F 1700.7 (8-72) Reproduction of completed page authorized (art.5/94)

DISCLAIMER

A University of Rhode Island (URI) research team prepared this report for the Rhode Island Department of Transportation (RIDOT). The contents of the report reflect the views of the URI research team, which is responsible for the accuracy of the facts and data presented herein. The contents are not to be construed as the official position of the RIDOT or URI. This document does not constitute a standard, specification or regulation.

Citation of trade or manufacturer's names does not constitute an official endorsement or approval of the use of such commercial products. Trade or manufacturer's names appear herein solely because they are considered essential to the object of this study.

PREFACE

This is the final report of the research project, entitled "Evaluation of Cracking and Permanent Deformation Resisting Characteristics of Recycled Asphalt Pavement (RAP) Binder." This study dealt with the investigation of the rheological properties of RAP binder to evaluate the resistance to permanent deformation and fatigue cracking using the Strategic Highway Research Program (SHRP) products, i.e., Superpave binder specification. In addition, this laboratory investigation characterized the fracture behavior and dynamic response of RAP binder and asphalt concrete. Results of this laboratory investigation help the engineers understand the resistance characteristics of asphalt binder containing RAP against permanent deformation and fatigue cracking of asphalt pavements. The report presents the results of:

1. Investigation of the relationship between rheological properties and RAP asphalt binder percentage for evaluation of the permanent deformation resistance characteristics;
2. Investigation of quasi-static behavior of asphalt binder containing RAP for the evaluation of permanent deformation resistance characteristics;
3. Investigation of the relationship between rheological properties and RAP asphalt binder percentage for evaluation of the fatigue cracking resistance characteristics;
4. Characterization of fracture toughness of the asphalt binder containing RAP binder; and
5. Characterization of the dynamic response of the asphalt binder containing RAP binder.

This research project was conducted by a research team of the College of Engineering at the University of Rhode Island (URI) under contract No. SPR-224-2235 (RIDOT-RTD-96-2) for the Rhode Island Department of Transportation (RIDOT). Funds were provided by RIDOT and the Federal Highway Administration (FHWA).

The work presented herein was accomplished by a team including Dr. K. Wayne Lee, Dr. Arun Shukla, Mr. Sanjiv Venkatram, and Mr. Nikone Soupharath. Appreciation is due to Messrs. Brian Gray, Amphone Soupharath, Sekhar Vajjhala, Eugene Mozzoni, and Sean Corrigan who assisted with laboratory work. Grateful recognition is forwarded to Mmes. Artie Martino and Virginia Mulholland for manuscript preparation and administrative assistance. The authors express their gratitude to Cardi Corporation and Lynch & Sons Inc., which supplied RAPs, and Hudson Co., which provided asphalt binders. The authors wish to acknowledge the assistance and cooperation of the RIDOT in this study. In particular, the authors are indebted to Messrs. Colin Franco, Francis Manning and Mrs. Deborah Munroe of Research and Technology Development section, and Messrs. Mark Felag, Mike Byrne, David Clark, William Ringgold and Mike Foisey of the Materials section.

TABLE OF CONTENTS

LIST OF TABLES

LIST OF FIGURES

1 INTRODUCTION

For over a century, paved roadways have been constructed using asphalt concrete mixtures in Rhode Island as well as across the United States. However, a major problem still exists in asphalt pavement involving premature distresses and failures, e.g., permanent deformation, fatigue cracking, and low temperature cracking.

Since asphalt binder is a thermoplastic material, its physical properties depend on temperature and time (Roberts et al. 1991). The physical properties of asphalt are a measure of its consistency. Since the early 1970s, many highway agencies have recycled old pavements in the overlay or major reconstruction. Recently, the use of Recycled Asphalt Pavement (RAP) has significantly increased due to the protection of the environment, economy of construction/rehabilitation procedures, and the conservation of materials. However, the evaluation of RAP performance has not been well established.

The Strategic Highway Research Program (SHRP) developed a performance-based specification for asphalt binder accompanied by a new system and testing procedures, as a component of "SUPERPAVE^{TM}," which stands for *Su*perior *Per*forming Asphalt *Pave*ment. Six types of new binder testing equipment were recommended to measure the physical properties of modified as well as unmodified asphalt binders that can be related directly to field performance by engineering principles. Among the equipment, the Dynamic Shear Rheometer (DSR) was chosen to evaluate permanent deformation and fatigue cracking resistance characteristics by measuring the properties of asphalt binder at high and intermediate temperatures, respectively. Yet, Superpave did not include the RAP mixture evaluation. Therefore, an attempt was made to evaluate RAP binder and mixtures utilizing

the Superpave tool and to help engineers gain insight into the use of RAP in asphalt pavement.

Since SHRP performed a limited investigation related to fracture and crack propagation within asphalt mixtures, further mechanical characterization of asphalt binder and mixture is warranted. In the present study, single notched specimens were used for the fracture toughness testing. Besides, split Hopkinson pressure bar (SHPB) equipment was utilized to characterize the dynamic constitutive behavior.

Specific objectives of the present study were:

1. To investigate the relationship between rheological properties and RAP asphalt binder percentage for evaluation of the permanent deformation resistance characteristics;
2. To investigate quasi-static behavior of asphalt binder containing RAP for the evaluation of permanent deformation resistance characteristics;
3. To investigate the relationship between rheological properties and RAP asphalt binder percentage for evaluation of the fatigue cracking resistance characteristics;
4. To characterize fracture toughness of the asphalt binder containing RAP binder;

2 PERMANENT DEFORMATION

Permanent deformation or rutting is a type of distress, which can be found in the surface of asphalt pavement. Rutting mostly occurs along the wheel path of the traffic. The surface cross section is no longer in its design position. It is caused by many sources (e.g., traffic densification, abrasion, and underlaying HMA weakened by moisture damage), and has two principal causes (May and McGennis 1996). Firstly, the rutting is caused by high stress being applied to the subgrade and/or granular subbase layer below the asphalt layer.

Secondly, the rutting results from the asphalt mixture having too low a shear strength to resist repeated heavy loads. Typically, rutting occurs during the hot summer under high pavement temperatures. Although aggregates play the major roles in causing permanent deformation, the soft asphalt binder can be contributing factor. Since rutting is an accumulation of very small permanent deformation, stiffer asphalt binder and mineral aggregates with a high degree of internal friction are needed to increase shear strength.

2.1 Rheological Properties by Dynamic Shear Rheometer (DSR)

2.1.1 *Experimental Plan*

Two base asphalts, i.e., AC-10 and AC-20, typically used in Rhode Island were blended with different amounts of RAP binders, i.e., 0, 10, 20, 30, 40, 50, 75 and 100%. DSR tests were performed at Superpave high-grade temperatures, i.e., 52, 58, 64, 70, and 76°C in accordance with the procedure of AASHTO TP5. These binders were aged using the rolling thin film oven (RTFO), and DSR tests were performed. Values of $G^*/\sin\delta$ were determined to evaluate the rutting resistance characteristics of binders for all temperatures. The overall experimental design is summarized in Table 2.1.

2.1.2 *Sample Preparation*

The RAPs were procured from two asphalt mixing plants (C and L) in Rhode Island. Then, RAP binders were recovered in accordance with the procedure of AASHTO T170-93 at the Rhode Island Department of Transportation (RIDOT) laboratory. It may be noted that information on the two RAP sources was not available. The base asphalts were procured from a Rhode Island distributor, H. Virgin and RAP asphalt binders were heated at 135°C and 160°C, respectively. The blended binders were aged in the RTFO system at 163°C, 15 rpm (carriage rotation), and 4,000 ml/min. (airflow rate) for 85 minutes to produce RTFO residue. Then, the absolute viscosity, rotational viscosity and DSR tests were performed on the unaged and RTFO aged binders.

2.1.3 *Laboratory Testing*

The absolute viscosity was measured at 60°C (140°F) in accordance with the procedure of AASHTO T202-91. The Brookfield rotational viscosity at 135°C was recommended in the Superpave binder specification to determine the handling and pumping characteristics of the asphalt binder at the refinery, terminal, or hot mixing asphalt plant. The test was performed in accordance with the procedure of ASTM D4402. An SC4-21 spindle was used for the base asphalt binders; and SC4-27 was used for the blended asphalt binders. Two samples for each blended asphalt binders were tested in the present study. The DSR was used to characterize the viscous and elastic behavior of asphalt binders. The test measures the complex shear modulus (G*) and phase angle (δ) of the asphalt binder at high and intermediate temperatures when the dynamic (oscillatory) shear is applied to the sample using parallel plate test geometry (McGennis et al. 1994). G* is a measure of the

total resistance of a material to deforming when repeatedly sheared. The δ is an indicator of the relative amounts of elastic (recoverable) and viscous (non-recoverable) deformation. The stress-strain response of asphalt binder at normal service temperature is shown in Figure 2.1.

The RTFO test was used to measure the effect of heat and air on the moving film of asphalt binders (Brown et al. 1996). This test was recommended in the Superpave binder specification to simulate short term aging during mixing at the plant and lay down process. According to the AASHTO Provisional Standard TP5, the unaged and RTFO aged asphalt binders were tested using the 25 mm plate and 1 mm gap setting. The unaged and RTFO aged asphalt binders are tested at 52, 58, 64, 70 and 76°C to determine G*/sinδ, the permanent deformation parameter. The high temperature grades are related to the average 7 days maximum pavement design temperature in Celsius in the United States. It may be noted that rutting typically occurs at high service temperature within the first two years after pavement construction.

2.1.4 *Test Results*

Table 2.2 shows the viscosity test results for the asphalt binders containing Plant C and L RAPs. The absolute viscosity increases as the amount of RAP increases as shown in Figures 2.2 and 2.3, respectively. Figures 2.4 and 2.5 show the rotational viscosity values versus RAP percentage for asphalt binder containing Plant C and L RAP, respectively. Both absolute and rotational viscosity values were plotted in a log-log scale on the Y-axis. The linear regression models and the coefficient of determination (R^2) were determined for AC-10 and AC-20 containing Plant C and L RAPs as shown in Table 2.7 and 2.8, respectively.

It may be noted that for rotational viscosity the calculation gives 10,000 times the tabulated value and that for dynamic shear the calculation gives 1,000 times the tabulated values. The models and high R^2 values of AC-10 and AC-20 containing Plant C and L RAP indicated the good linear relationship between the viscosity as a function of RAP amount in asphalt binder. The viscosity values of Plant C RAP binder were lower than the ones of Plant L RAP binder, and implies that the latter RAP binder is harder than the former (Figures 2.4 and 2.5). The characteristic of RAP binder is dependent on the age of the RAP. The older the RAP, the harder the RAP binder due to the volatilization and oxidation. However, the age of RAP was not available, because the original sources of the RAP were not identifiable. The Superpave binder specification requires that the rotational viscosity at 135°C be less than 3 Pa-s. The viscosity values for some RAP binder contents do not meet the requirement.

A constant stress mode was used for the DSR test in the present study. The rutting parameter, $G^*/\sin\delta$ was measured at 52, 58, 64, 70, and 76°C. Tables 2.3 through 2.6 show the DSR test results of asphalt binder containing Plant C and L RAPs, respectively. The experimental data were also plotted for the comparative analysis purpose as show in Figures 2.6 through 2.13. It may be noted that the Y-axis is in a log-log scale. Table 2.7 and 2.8 show the linear regression models and the R^2 values for the unaged and RTFO aged asphalt binder.

2.1.5 *Analysis and Discussion*

The Superpave binder specification requires the rutting factor, $G^*/\sin\delta$ to be a minimum of 1.00 kPa and 2.20 kPa for unaged and RTFO aged binders, respectively. The

rutting factor reflects the total resistance of a binder to deform under repeated loading (G*), and the relative energy dissipated into non-recoverable deformation (sinδ) during the loading cycle. A higher value of G*/sinδ implies that the binder behaves more like an elastic material, which is desirable for rutting resistance. Since G*/sinδ for unaged binder requires a minimum of 1.00 kPa to resist tenderness during the lay down process in the field, these values were not considered seriously. Rather, the rutting resistance was evaluated mainly by examining G*/sinδ values of RTFO aged binders, because the aged binder simulated plant aging.

As expected, the values of G*/sinδ for unaged and RTFO aged binders were increased as the content of RAP binder was increased at all temperatures (Figures 2.6 through 2.13). It was also observed that the binder with Plant L RAP exhibited higher G*/sinδ values than the one with Plant C RAP at all corresponding temperatures. It may be noted that the slope for binder with Plant L RAP is stiffer than the one for binder with Plant C RAP.

The high temperature grading of AC-10 used in the present study was 58; and the values of G*/sinδ for RTFO aged binder was evaluated in Figure 2.10 and 2.11. It was noticed that all values at 58°C were higher than the minimum 2.2 kPa. Similarly, Figure 2.12 and 2.13 show that all values at 64°C for RTFO aged binder of AC-20 asphalt exhibited higher than the minimum requirement. From the linear regression analysis at high temperatures, it was observed that all R^2 values were observed above 0.90, except for AC-10 containing Plant C-RAP at 52°C was observed to be above 0.87. Again, this shows the good relationship between the stiffness of the asphalt binder and RAP content. It may be noted that the y-intercept values were set on the stiffness values at 0% RAP.

2.2 Quasi-Static Characterization Experiments with Uniaxial Compression Test

The quasi-static experiments were conducted in accordance with ASTM D1074-93 to determine the compressive strength of the binders. The specimen was cylindrical in shape with 4 inches in diameter and 2 inches height.

The specimens were fabricated using the Marshall Compactor (Asphalt Institute 1993). The aggregates used for this study were of size -#30+#50 and were procured from two different contractors, i.e., contractors T and C. The aggregate size was so chosen that the aggregate would not contribute to the strength of the specimen and only binder characteristics could be studied (Kennedy et al. 1982). The virgin asphalt cement used was AC-20. The RAP was obtained from Plant C, and the RAP binder was extracted and recovered. The compaction procedure was in accordance with Kennedy et al. (1982). The heated mix of the binder and aggregates was compacted using the Instron testing machine under a uniaxial load of 6,000 lbs for 15 minutes. The compacted specimen was later ejected and cured overnight before testing.

2.2.1 *Quasi-Static Behavior of Virgin Asphalt and RAP Binders*

The specimens were tested in axial compression without lateral support at a uniform rate of vertical displacement of 0.05 in./min-in (1.25 mm/min-mm), i.e., for the present study at 0.1 in/min (2.5 mm/min). The displacement as a function of the load was recorded using a two-channel data acquisition system, the NICOLET. As per the standards, three specimen each were tested at each increment in RAP content and the average of the results was taken as the compressive strength of the sample, at the corresponding RAP percentage.

The results from this study are presented in Table 2.9 and the average results from

experiments are provided in Figure 2.14. A perceivable increase of over 100% was noticed in both stiffness (E) and σ_u for the 75% RAP and 100% RAP specimen. The addition of 25%RAP to the virgin binder increased the Young's modulus and compressive strength by 26%. The incremental addition to 50% RAP increased the modulus marginally (8%) but increased the compressive strength by 31%. The addition of RAP however, did not cause a noticeable variation in the yield strain of the virgin binder. An aspect to note is the steady increase in the linear range of the stress-strain response when RAP content is increased in the binders as shown in Figure 2.14.

The mechanism of failure in all the specimens was noticed to be shear dominated, as shown in Figure 2.15. The side view is indicative of shear failure in the specimen, wherein the wedge shaped segments have been removed from the central core. The angle of shear happens to be approximately 45^0. This was observed in all the specimens, irrespective of the RAP content in them. The top view of 100% RAP specimen (Figure 2.16) shows the presence of circumferential cracks and also the formation of different segments along the periphery of the specimen.

Figures 2.17 and 2.18 show the presence of longitudinal cracks in all the specimens that were tested. These cracks presumably have been caused due to the circumferential stresses $\sigma_{\theta\theta}$, thus splitting the surface of the specimen lengthwise. These circumferential stresses may have been caused because of frictional effects, leading to a complex stress state along the periphery of the specimen. The cracks were observed to be much more predominant as the RAP content was increased, much unlike the presence of smaller cracks in the 0% RAP specimen. The cracks then proceeded inwards and due to maximum shear stress occurring along those planes, led to the formation of the wedge shaped segments.

Also it appears that the number of these wedge shaped segments decreased as the RAP content increased. The low stiffness and the observation of crack propagation indicate a large amount of ductility in the virgin binder. However, it is apparent that the addition of RAP is causing the stiffness to increase, thus causing the binder to behave in a brittle manner.

TABLE 2.1 OVERALL EXPERIMENTAL DESIGN

(a) Experimental Design for RAP Binder Testing in Accordance with Superpave Specification.

Tests	RAP,%							
	0	10	20	30	40	50	75	100
Absolute viscosity	4	4	4	4	4	4	4	4
DSR, Unaged	4	4	4	4	4	4	4	4
DSR, RTFO	4	4	4	4	4	4	4	4
DSR, PAV	4	4	4	4	4	4	4	4

Note: 1. 2 (RAP source) x 2 (AC-20 & AC-10) = 4

2. All DSR testing was performed at the Superpave high temperature grade temperatures (52, 58, 64, 70, and 76°C).

(b) Experimental Design for Mechanical Properties.

Tests	RAP,%				
	0	25	50	75	100
Comp. Strength	3	3	3	3	3
Fracture	5	5	5	5	5
SHPB	2	2	2	2	2

Note: AC-20 base asphalt binder with Plant C RAP.

Table 2.2 Absolute and Rotational Viscosity Results of Asphalt Binders Containing RAP.

RAP, %	Absolute Viscosity Values at 60°C, (Poise)		Rotational Viscosity Values at 135°C, (Pa-s)	
	AC-10 (PG 58-22)	AC-20 (PG 64-22)	AC-10 (PG 58-22)	AC-20 (PG 64-22)
RAP from Plant C				
0	1,035	2,209	0.302	0.393
10	1,225	2,623	0.350	0.409
20	1,625	2,864	0.394	0.434
30	2,133	3,241	0.425	0.507
40	2,700	4,446	0.488	0.592
50	3,902	5,769	0.581	0.688
75	10,011	12,033	0.834	0.982
100	18,640	18,640	1.124	1.124
RAP from Plant L				
0	1,035	2,209	0.302	0.393
10	1,689	3,383	0.378	0.486
20	3,114	5,146	0.444	0.567
30	4,303	6,672	0.544	0.706
40	7,453	14,422	0.682	0.800
50	13,170	19,965	0.850	1.044
75	77,818	103,165	1.600	1.700
100	463,836	463,836	3.694	3.694

Table 2.3 DSR Test Results of Unaged Asphalt Binders Containing Plant C-RAP.

RAP, %	Temps, C	Unaged					
		AC 10			AC 20		
		G*	δ	G*/sinδ	G*	δ	G*/sinδ
0	52	3.14	83.2	3.16	-	-	-
	58	1.47	86.6	1.47	2.19	86.1	2.20
	64	0.78	87.7	0.78	1.13	87.2	1.13
	70	0.42	88.7	0.42	0.61	88.0	0.61
	76	-	-	-	-	-	-
10	52	3.54	83.3	3.56	8.34	82.2	8.42
	58	1.57	86.0	1.57	3.55	84.1	3.57
	64	0.98	86.6	0.98	1.71	86.1	1.71
	70	0.59	87.8	0.59	0.81	87.5	0.81
	76	0.31	88.8	0.31	0.42	88.5	0.42
20	52	5.80	82.1	5.86	-	-	-
	58	2.63	84.0	2.64	3.91	83.3	3.94
	64	1.28	85.6	1.28	1.77	85.7	1.77
	70	0.66	87.0	0.66	0.89	86.7	0.89
	76	-	-	-	-	-	-
30	52	-	-	-	-	-	-
	58	3.23	82.4	3.26	4.39	82.3	4.43
	64	1.54	84.8	1.55	2.05	84.6	2.06
	70	0.79	86.2	0.79	1.02	86.2	1.02
	76	0.47	87.5	0.47	0.50	87.6	0.5
40	52	-	-	-	-	-	-
	58	3.52	81.9	3.56	6.36	80.6	6.45
	64	1.67	84.3	1.68	2.84	83.5	2.86
	70	0.84	85.7	0.84	1.41	85.3	1.41
	76	0.48	87.1	0.48	0.69	86.6	0.69
50	52	-	-	-	-	-	-
	58	3.59	81.0	3.63	6.76	79.7	6.87
	64	1.75	83.4	1.76	3.12	82.1	3.15
	70	0.86	85.1	0.86	1.48	84.3	1.49
	76	0.48	86.5	0.48	0.75	86.1	0.75
75	52	-	-	-	27.09	72.1	28.47
	58	6.20	77.5	6.35	13.06	75.8	13.47
	64	2.99	80.7	3.03	5.47	79.1	5.57
	70	1.47	82.8	1.48	2.67	81.8	2.7
	76	0.74	85.3	0.74	1.28	84.4	1.29
100	52	-	-	-	-	-	-
	58	-	-	-	-	-	-
	64	8.49	75.3	8.78	8.49	75.3	8.78
	70	4.04	78.4	4.12	4.04	78.4	4.12
	76	1.95	81.5	1.97	1.95	81.5	1.97

Note: - indicated that the data is not available.

Table 2.4 DSR Test Results of RTFO aged Asphalt Binders Containing Plant C-RAP.

RAP, %	Temps, C	RTFO Aged					
		AC 10			AC 20		
		G*	δ	G*/sinδ	G*	δ	G*/sinδ
0	52	7.55	80.4	7.66	-	-	-
	58	3.60	82.6	3.63	6.01	81.2	6.08
	64	1.89	84.6	1.90	2.69	83.9	2.71
	70	0.91	86.3	0.91	1.47	85.8	1.47
	76	-	-	-	-	-	-
10	52	8.45	78.4	8.63	-	-	-
	58	3.86	81.5	3.90	7.05	80.9	7.14
	64	1.99	83.6	2.00	3.36	83.4	3.38
	70	0.97	85.7	0.97	1.73	85.3	1.74
	76	0.51	87.1	0.51	-	-	-
20	52	13.72	75.3	14.18	-	-	-
	58	6.25	78.3	6.38	11.68	78.0	11.94
	64	2.93	81.4	2.96	4.83	80.8	4.89
	70	1.43	83.8	1.44	2.33	83.3	2.35
	76	-	-	-	1.16	85.4	1.16
30	52	-	-	-	-	-	-
	58	11.09	76.0	11.43	13.96	75.6	14.41
	64	4.89	79.3	4.98	6.25	78.8	6.37
	70	2.46	81.9	2.48	3.04	81.9	3.07
	76	1.39	83.9	1.40	1.44	84.3	1.45
40	52	-	-	-	-	-	-
	58	15.73	72.8	16.47	19.64	73.2	20.52
	64	7.35	75.9	7.58	8.69	77.0	8.92
	70	3.60	79.2	3.66	4.25	80.0	4.32
	76	1.85	81.9	1.87	1.96	82.9	1.98
50	52	48.52	67.0	52.71	-	-	-
	58	21.38	70.7	22.65	25.91	70.2	27.54
	64	9.77	74.8	10.12	12.45	74.2	12.94
	70	4.54	78.4	4.63	6.06	77.8	6.2
	76	2.17	81.6	2.19	2.75	80.9	2.79
75	52	-	-	-	99.51	62.0	112.7
	58	-	-	-	47.62	65.7	52.25
	64	10.84	72.9	11.34	21.26	69.8	22.65
	70	5.15	76.3	5.30	8.32	73.7	8.67
	76	2.60	79.6	2.64	5.02	77.2	5.15
100	52	-	-	-	-	-	-
	58	-	-	-	-	-	-
	64	37.72	70.8	39.94	37.72	70.8	39.94
	70	10.45	72.3	10.97	10.45	72.3	10.97
	76	8.45	73.6	8.81	8.45	73.6	8.81

Note: - indicated that the data is not available.

Table 2.5 DSR Test Results of Unaged Asphalt Binders Containing Plant L-RAP.

RAP, %	Temps, C	Unaged					
		AC 10			AC 20		
		G*	δ	G*/sinδ	G*	δ	G*/sinδ
0	52	3.14	83.2	3.16	-	-	-
	58	1.47	86.6	1.47	2.19	86.1	2.20
	64	0.78	87.7	0.78	1.13	87.2	1.13
	70	0.42	88.7	0.42	0.61	88.0	0.61
	76	-	-	-	-	-	-
10	52	3.72	84.0	3.74	10.32	80.8	10.45
	58	1.65	85.9	1.65	4.71	83.1	4.74
	64	1.15	87.2	1.15	2.01	84.8	2.02
	70	0.39	87.7	0.39	1.01	87.0	1.01
	76	0.21	88.7	0.21	0.51	88.0	0.51
20	52	7.57	80.5	7.68	17.14	77.5	17.56
	58	3.05	82.8	3.07	7.24	80.5	7.34
	64	1.47	85.2	1.48	3.26	82.4	3.29
	70	0.72	86.3	0.72	1.50	85.0	1.51
	76	0.38	87.4	0.38	0.76	86.4	0.76
30	52	12.52	77.4	12.83	23.36	74.9	24.20
	58	5.08	80.4	5.15	10.94	77.9	11.19
	64	2.11	83.1	2.13	4.74	80.9	4.80
	70	1.17	85.1	1.17	2.20	83.1	2.22
	76	0.58	86.9	0.58	1.12	85.6	1.12
40	52	18.59	74.0	19.34	32.43	71.5	34.20
	58	8.11	77.0	8.32	15.67	75.0	16.22
	64	3.56	80.2	3.61	6.39	77.2	6.55
	70	1.53	83.7	1.54	2.94	80.0	2.99
	76	0.85	85.2	0.85	1.52	82.5	1.53
50	52	29.60	71.0	31.31	37.93	69.9	40.39
	58	13.13	74.8	13.61	16.48	73.6	17.18
	64	5.64	77.7	5.77	8.31	76.7	8.54
	70	2.56	80.9	2.59	3.70	79.6	3.76
	76	1.27	83.6	1.28	1.79	82.6	1.80
75	52	83.67	62.7	94.16	68.89	63.3	77.11
	58	38.06	65.5	41.83	31.53	66.7	34.33
	64	18.71	69.2	20.01	15.76	71.1	16.66
	70	8.71	72.7	9.12	7.28	74.9	7.54
	76	4.25	76.5	4.37	3.43	78.1	3.51
100	52	251.08	52.7	315.63	251.08	52.7	315.63
	58	121.29	56.3	145.79	121.29	56.3	145.79
	64	59.83	61.9	67.83	59.83	61.9	67.83
	70	28.17	65.0	31.08	28.17	65.0	31.08
	76	13.60	68.9	14.58	13.60	68.9	14.58

Note: - indicated that the data is not available.

Table 2.6 DSR Test Results of RTFO aged Asphalt Binders Containing Plant L-RAP.

RAP, %	Temps, C	RTFO Aged					
		AC 10			AC 20		
		G*	δ	G*/sinδ	G*	δ	G*/sinδ
0	52	7.55	80.4	7.66	-	-	-
	58	3.60	82.6	3.63	6.01	81.2	6.08
	64	1.89	84.6	1.90	2.69	83.9	2.71
	70	0.91	86.3	0.91	1.47	85.8	1.47
	76	-	-	-	-	-	-
10	52	10.92	77.4	11.19	19.38	75.7	20.00
	58	4.94	80.8	5.00	8.92	80.0	9.06
	64	2.18	83.4	2.19	3.86	81.7	3.90
	70	1.05	85.4	1.05	1.84	83.9	1.85
	76	0.54	86.4	0.54	0.93	85.9	0.93
20	52	20.47	72.5	21.46	25.57	72.5	26.81
	58	8.09	76.3	8.33	11.85	76.4	12.19
	64	3.86	79.9	3.92	5.48	79.6	5.57
	70	1.80	82.5	1.82	2.42	82.2	2.44
	76	0.90	84.6	0.90	1.23	84.5	1.24
30	52	36.21	67.5	39.19	49.07	67.9	52.96
	58	15.98	71.7	16.83	21.20	71.5	22.35
	64	7.80	75.1	8.07	7.29	75.0	7.55
	70	3.53	78.6	3.60	4.36	78.4	4.45
	76	1.70	81.6	1.72	2.10	81.5	2.12
40	52	66.62	63.2	74.64	102.47	61.6	116.49
	58	29.28	66.7	31.88	46.60	64.6	51.59
	64	13.73	70.5	14.57	21.90	68.4	23.55
	70	6.02	74.3	6.25	10.72	71.6	11.30
	76	2.88	78.0	2.94	5.19	75.9	5.35
50	52	83.69	60.1	96.54	113.16	60.4	130.14
	58	37.69	63.6	42.08	52.58	63.1	58.96
	64	17.89	68.1	19.28	25.87	67.0	28.10
	70	9.02	71.6	9.51	11.45	71.1	12.10
	76	4.36	75.7	4.50	6.04	75.0	6.25
75	52	201.89	54.1	249.23	322.59	55.0	393.81
	58	80.45	47.1	109.82	142.74	55.2	173.83
	64	45.82	61.2	52.29	71.61	59.2	83.37
	70	22.26	65.6	24.44	36.24	62.8	40.75
	76	10.86	69.4	11.60	17.17	67.2	18.63
100	52	386.63	44.5	551.61	386.63	44.5	551.61
	58	181.21	51.3	232.19	181.21	51.3	232.19
	64	89.11	56.0	107.49	89.11	56.0	107.49
	70	45.81	60.0	52.90	45.81	60.0	52.90
	76	23.11	63.8	25.76	23.11	63.8	25.76

Note: - indicated that the data is not available.

Table 2.7 The Linear Regression Models and Coefficient of Determinations (R^2) for Plant C RAP.

RAP from Plant C			
Dependent Parameter, Y	**Temperature, (°C)**	**AC-10 (PG 58-22)**	**AC-20 (PG 64-22)**
Absolute Viscosity	60	$Y = 0.4793 + 0.001530X$ $R^2 = 0.9931$	$Y = 0.5243 + 0.001050X$ $R^2 = 0.9771$
Rotational Viscosity	135	$Y = 0.5416 + 0.0006674X$ $R^2 = 0.9965$	$Y = 0.5556 + 0.0005396X$ $R^2 = 0.9692$
G*/sinδ determined by DSR test for unaged binder	52	$Y = 0.5440 + 0.001412X$ $R^2 = 0.8709$	-
	58	$Y = 0.5007 + 0.001127X$ $R^2 = 0.919$	$Y = 0.5241 + 0.001275X$ $R^2 = 0.9437$
	64	$Y = 0.4612 + 0.001229X$ $R^2 = 0.9602$	$Y = 0.4847 + 0.001172X$ $R^2 = 0.9704$
	70	$Y = 0.4188 + 0.001259X$ $R^2 = 0.9417$	$Y = 0.4449 + 0.001172X$ $R^2 = 0.9878$
	76	$Y = 0.3799 + 0.001234X$ $R^2 = 0.9171$	$Y = 0.4037 + 0.001148X$ $R^2 = 0.9871$
G*/sinδ determined by DSR test for RTFO aged binder	52	$Y = 0.5893 + 0.001272X$ $R^2 = 0.8706$	-
	58	$Y = 0.5514 + 0.001754X$ $R^2 = 0.9617$	$Y = 0.5779 + 0.001401X$ $R^2 = 0.9842$
	64	$Y = 0.5157 + 0.001467X$ $R^2 = 0.9473$	$Y = 0.5257 + 0.001368X$ $R^2 = 0.9809$
	70	$Y = 0.4712 + 0.001480X$ $R^2 = 0.9115$	$Y = 0.5007 + 0.001224X$ $R^2 = 0.9312$
	76	$Y = 0.4370 + 0.001565X$ $R^2 = 0.9070$	$Y = 0.4614 + 0.001394X$ $R^2 = 0.9893$

Note: 1. Independent variable, X indicates the amount of RAP in asphalt binder.
2. - indicates that the data is not enough to develop the linear regression model .

Table 2.8 The Linear Regression Models and Coefficient of Determinations (R^2) for Plant L RAP.

RAP from Plant L			
Dependent Parameter, Y	**Temperature, (°C)**	**AC-10 (PG 58-22)**	**AC-20 (PG 64-22)**
Absolute Viscosity	60	$Y = 0.4793 + 0.002759X$ $R^2 = 0.9982$	$Y = 0.5243 + 0.002283X$ $R^2 = 0.9962$
Rotational Viscosity	135	$Y = 0.5416 + 0.001123X$ $R^2 = 0.9933$	$Y = 0.5556 + 0.0009918X$ $R^2 = 0.9932$
G*/sinδ determined by DSR test for unaged binder	52	$Y = 0.5440 + 0.002042X$ $R^2 = 0.9885$	$Y = 0.5926 + 0.001383X$ $R^2 = 0.9790$
	58	$Y = 0.5007 + 0.002177X$ $R^2 = 0.9911$	$Y = 0.5241 + 0.001995X$ $R^2 = 0.8974$
	64	$Y = 0.4612 + 0.002244X$ $R^2 = 0.9977$	$Y = 0.4847 + 0.002077X$ $R^2 = 0.9457$
	70	$Y = 0.4188 + 0.002302X$ $R^2 = 0.9800$	$Y = 0.4449 + 0.002114X$ $R^2 = 0.9660$
	76	$Y = 0.3528 + 0.002737X$ $R^2 = 0.9923$	$Y = 0.4193 + 0.001927X$ $R^2 = 0.9825$
G*/sinδ determined by DSR test for RTFO aged binder	52	$Y = 0.5893 + 0.001910X$ $R^2 = 0.9415$	$Y = 0.6287 + 0.001457X$ $R^2 = 0.9322$
	58	$Y = 0.5514 + 0.001996X$ $R^2 = 0.9509$	$Y = 0.5779 + 0.001766X$ $R^2 = 0.9307$
	64	$Y = 0.5157 + 0.002063X$ $R^2 = 0.9561$	$Y = 0.5257 + 0.001926X$ $R^2 = 0.9302$
	70	$Y = 0.4712 + 0.002235X$ $R^2 = 0.9631$	$Y = 0.5007 + 0.001985X$ $R^2 = 0.9399$
	76	$Y = 0.4333 + 0.002228X$ $R^2 = 0.9600$	$Y = 0.4649 + 0.002019X$ $R^2 = 0.9271$

Note: 1. Independent variable, X indicates the amount of RAP in asphalt binder.

Table 2.9 Result of Static Characterization Study with AC-20 Base Binder with Plant C RAP.

RAP, %	Compressive Strength, kPa				Yield Strain, %				Stiffness, kPa
	Trial 1	Trial 2	Trial 3	Average	Trial 1	Trial 2	Trial 3	Average	
0	53.6	52.1	-	52.9	17	16	-	16.5	470
25	70.2	69.2	61.1	66.8	16	19	17	17.3	593
50	87.8	87.5	87.6	87.6	17	16	16	16.3	640
75	123.8	109.9	115	116.2	18	19	19	18.7	954
100	123.9	124.5	124.5	124.3	18	18	19	18.3	976

Note: - indicated that the data is not available.

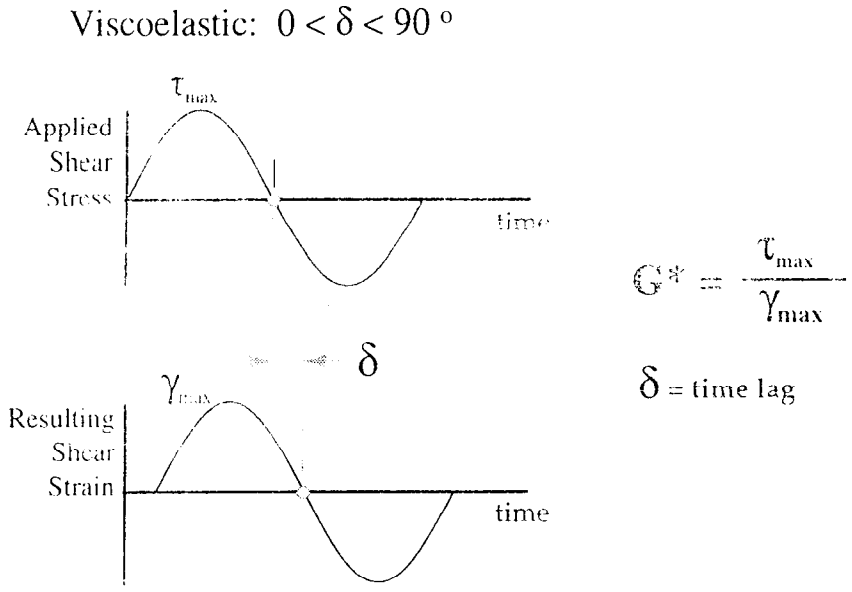

Figure 2.1 Stress-Strain Response of a Viscoelastic Material.

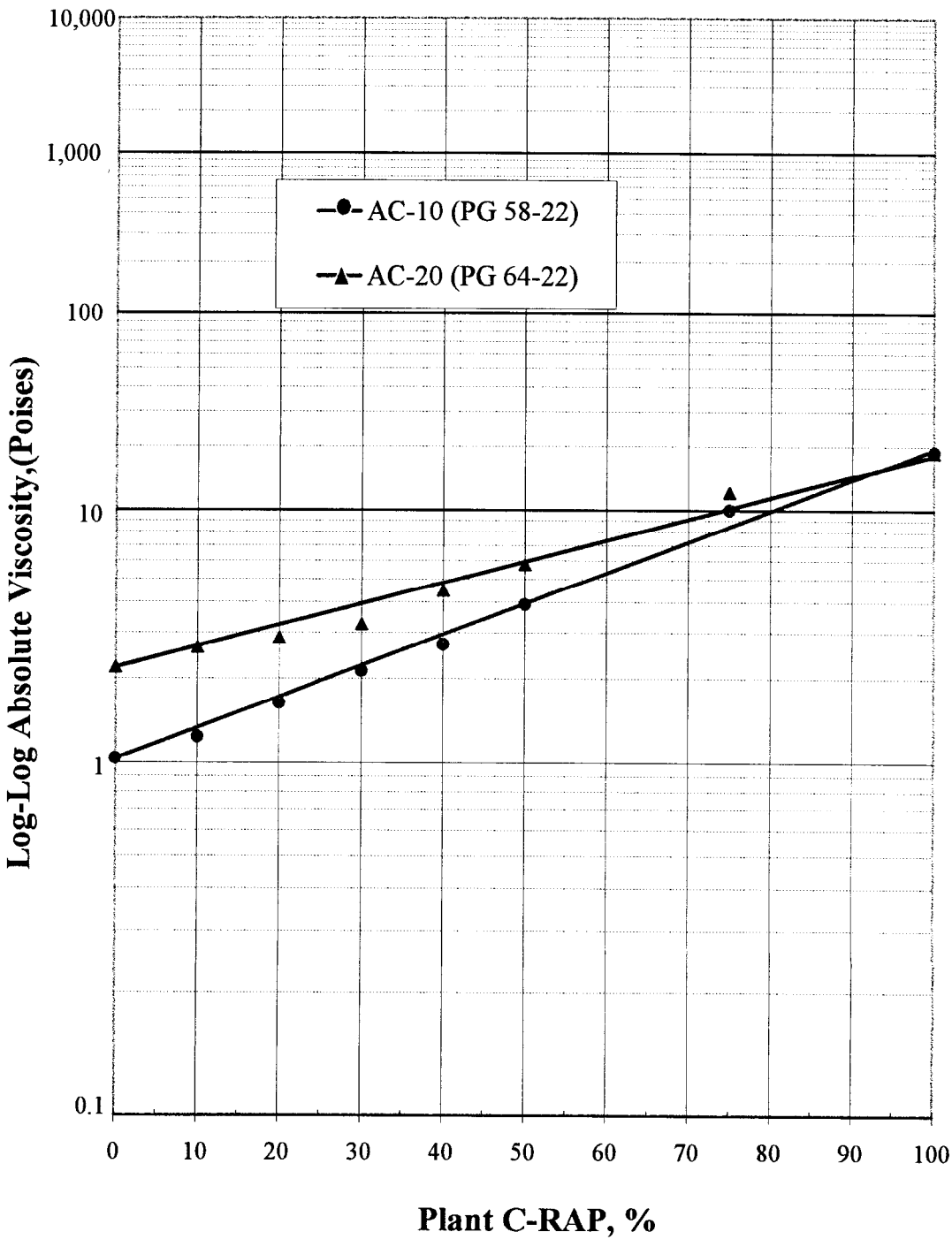

Figure 2.2. Absolute Viscosity Values at 60 C of Asphalt Binders Containing Plant C-RAP.

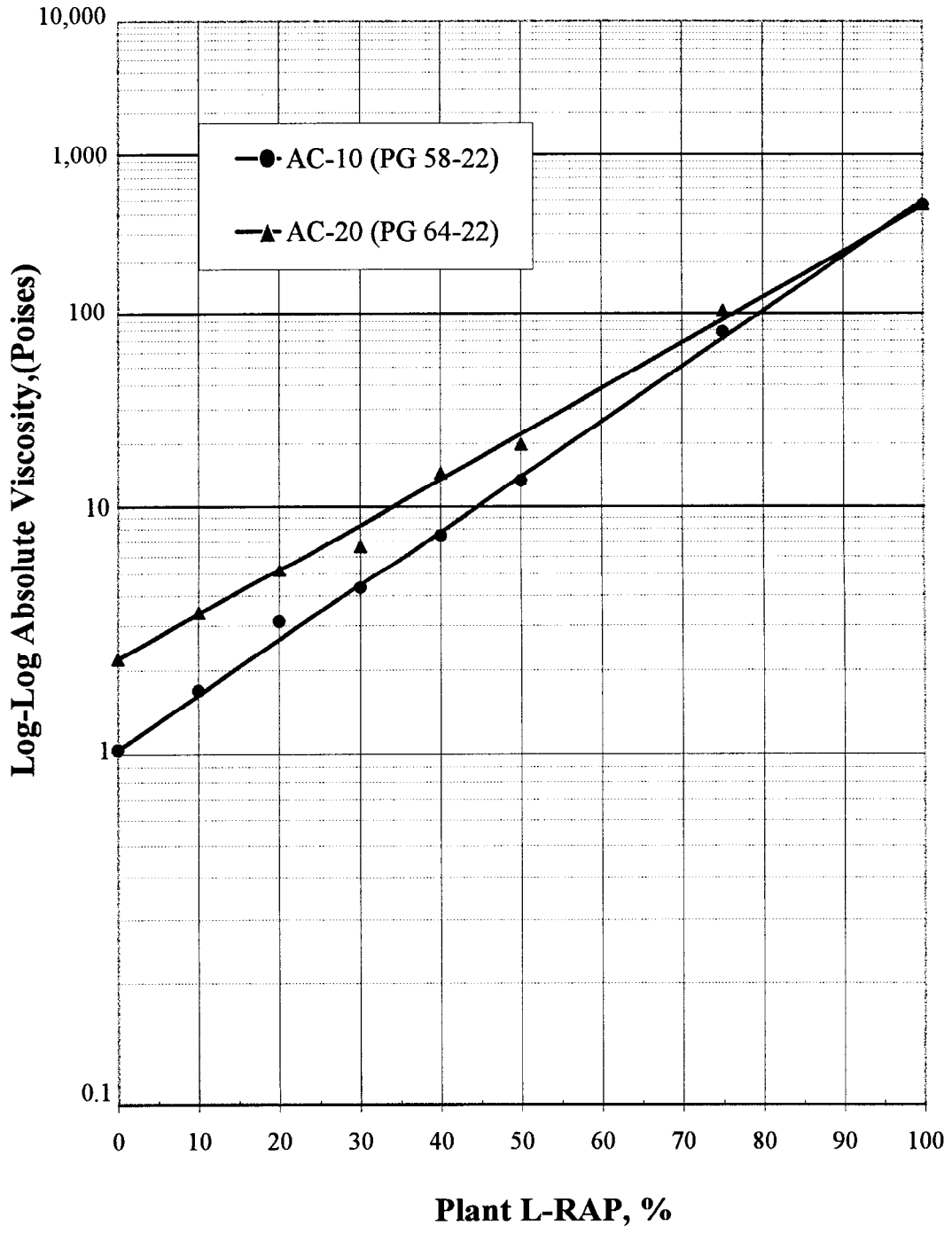

Figure 2.3. Absolute Viscosity Values at 60 C of Asphalt Binders Containing Plant L-RAP.

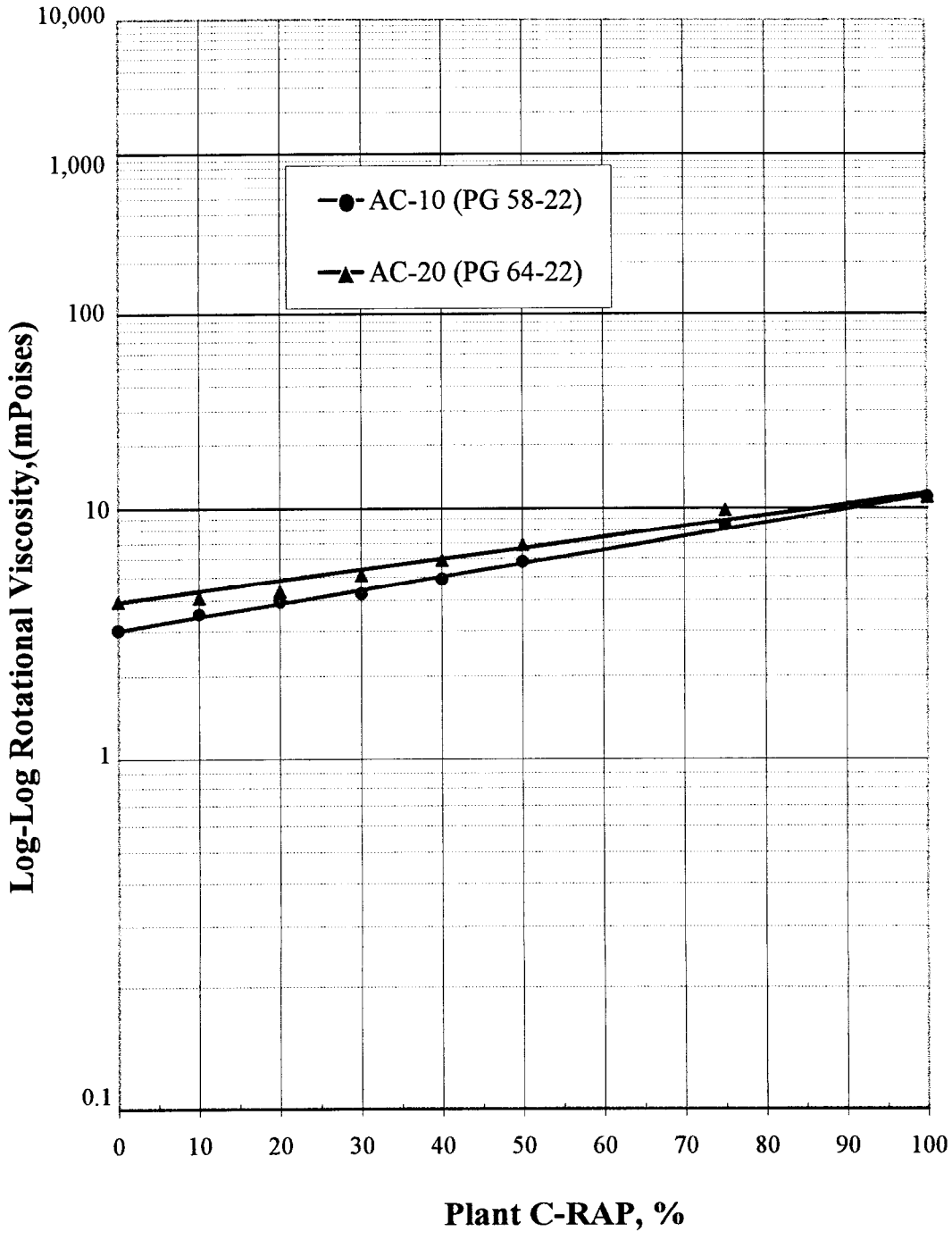

Figure 2.4. Rotational Viscosity Values at 135 C of Asphalt Binders Containing Plant C-RAP.

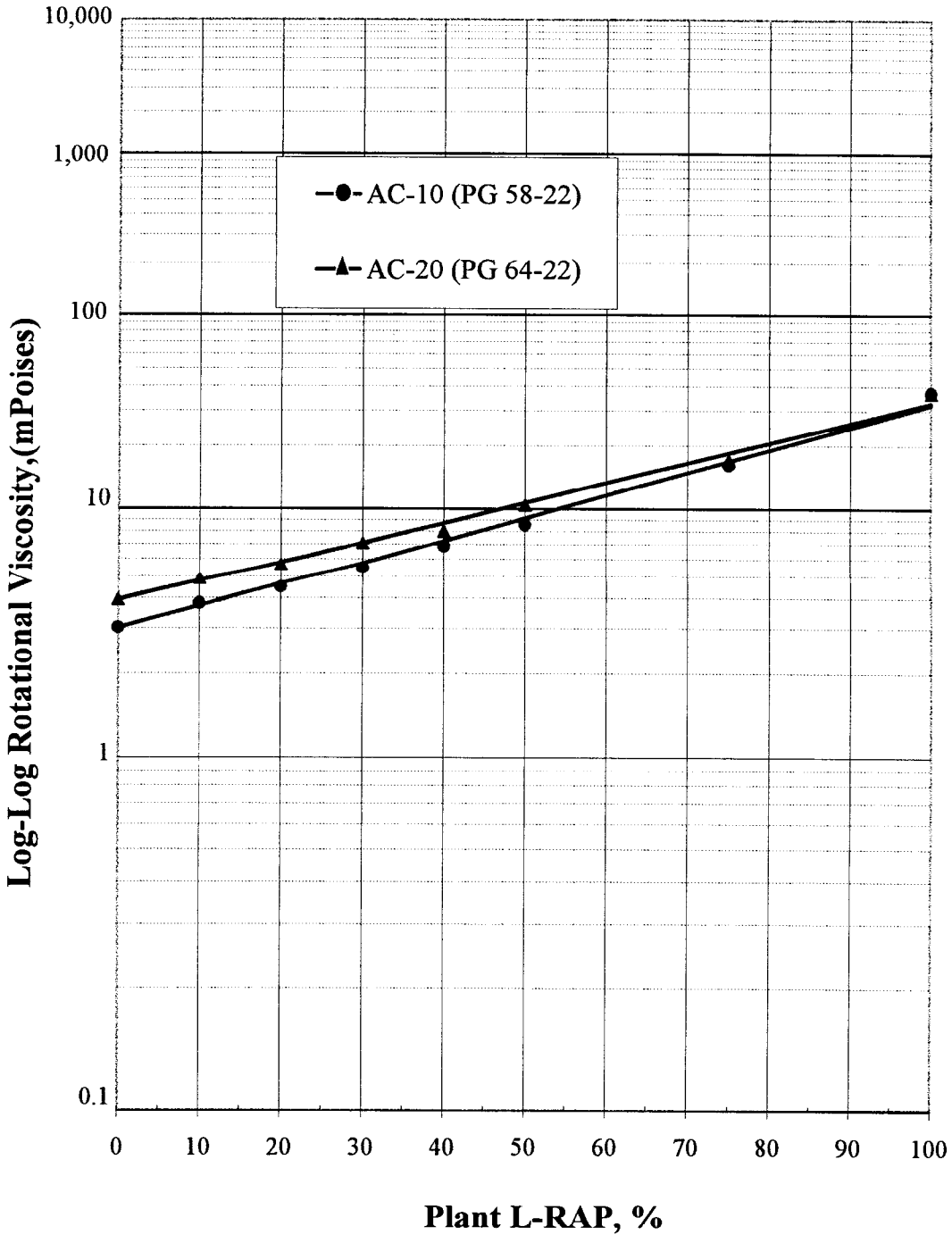

Figure 2.5. Rotational Viscosity Values at 135 C of Asphalt Binders Containing Plant L-RAP.

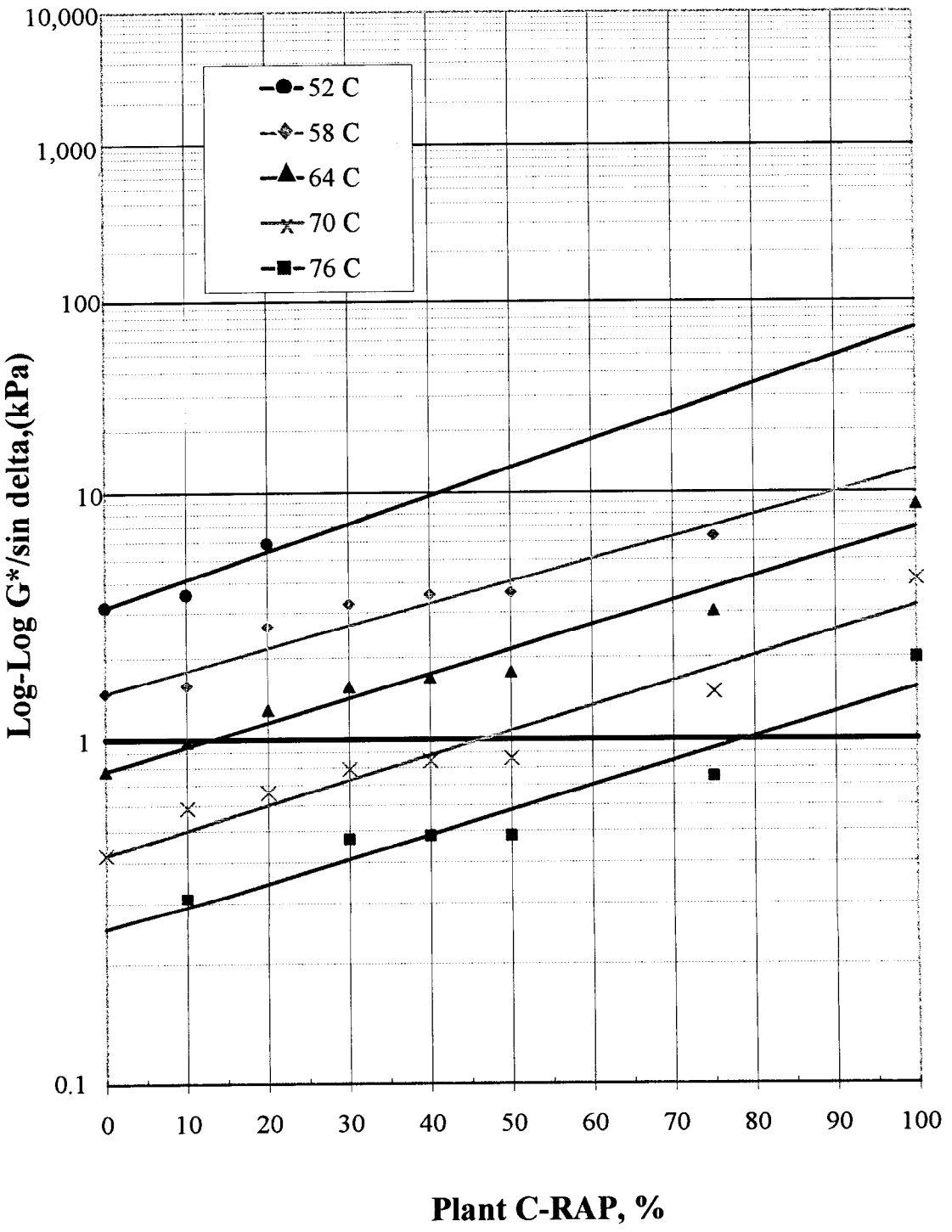

Figure 2.6. Comparison of DSR Test Results for Unaged Binder of AC-10 (PG 58-22) Base Binder Containing Plant C-RAP at Different Temperatures.

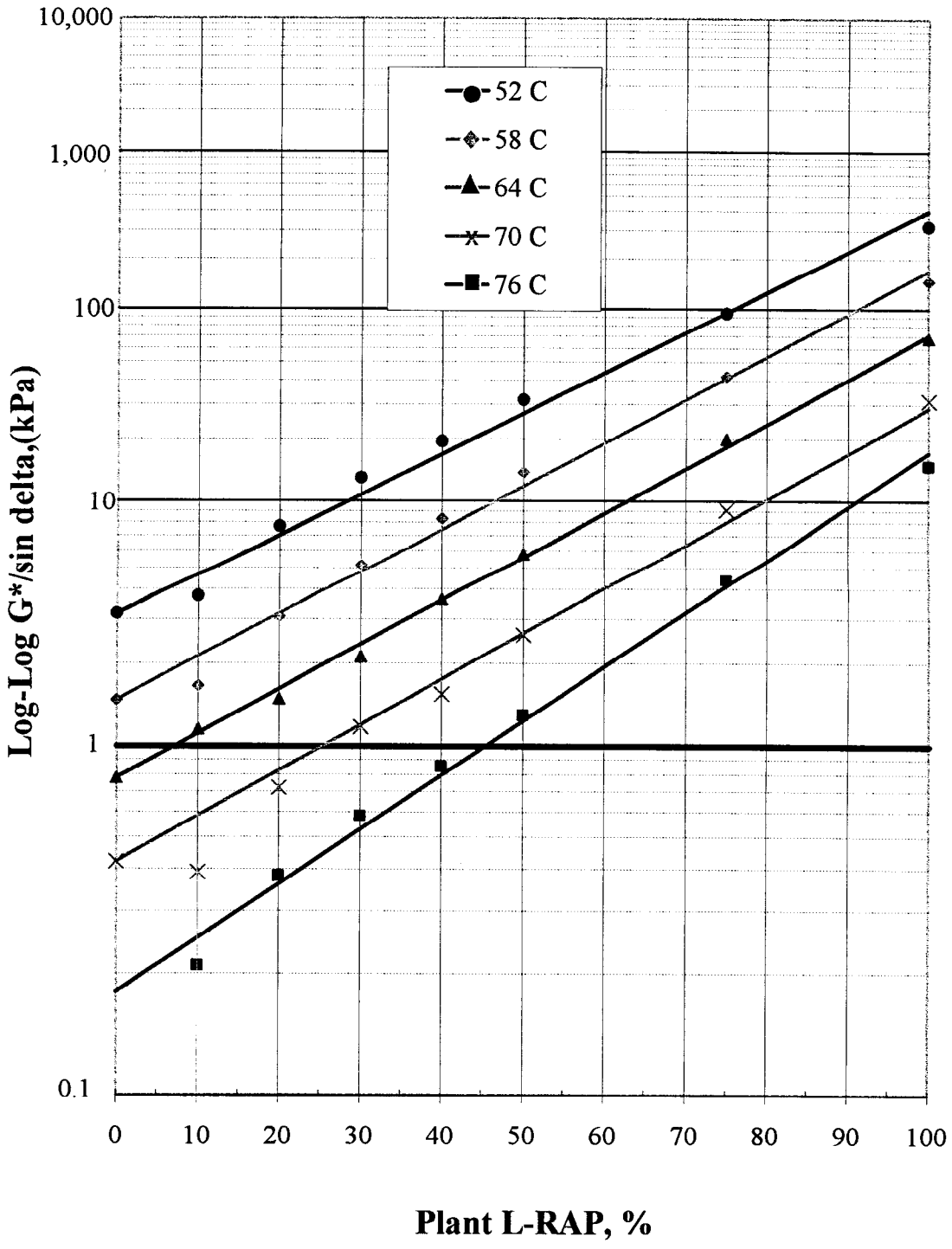

Figure 2.7. Comparison of DSR Test Results for Unaged Binder of AC-10 (PG 58-22) Base Binder Containing Plant L-RAP at Different Temperatures.

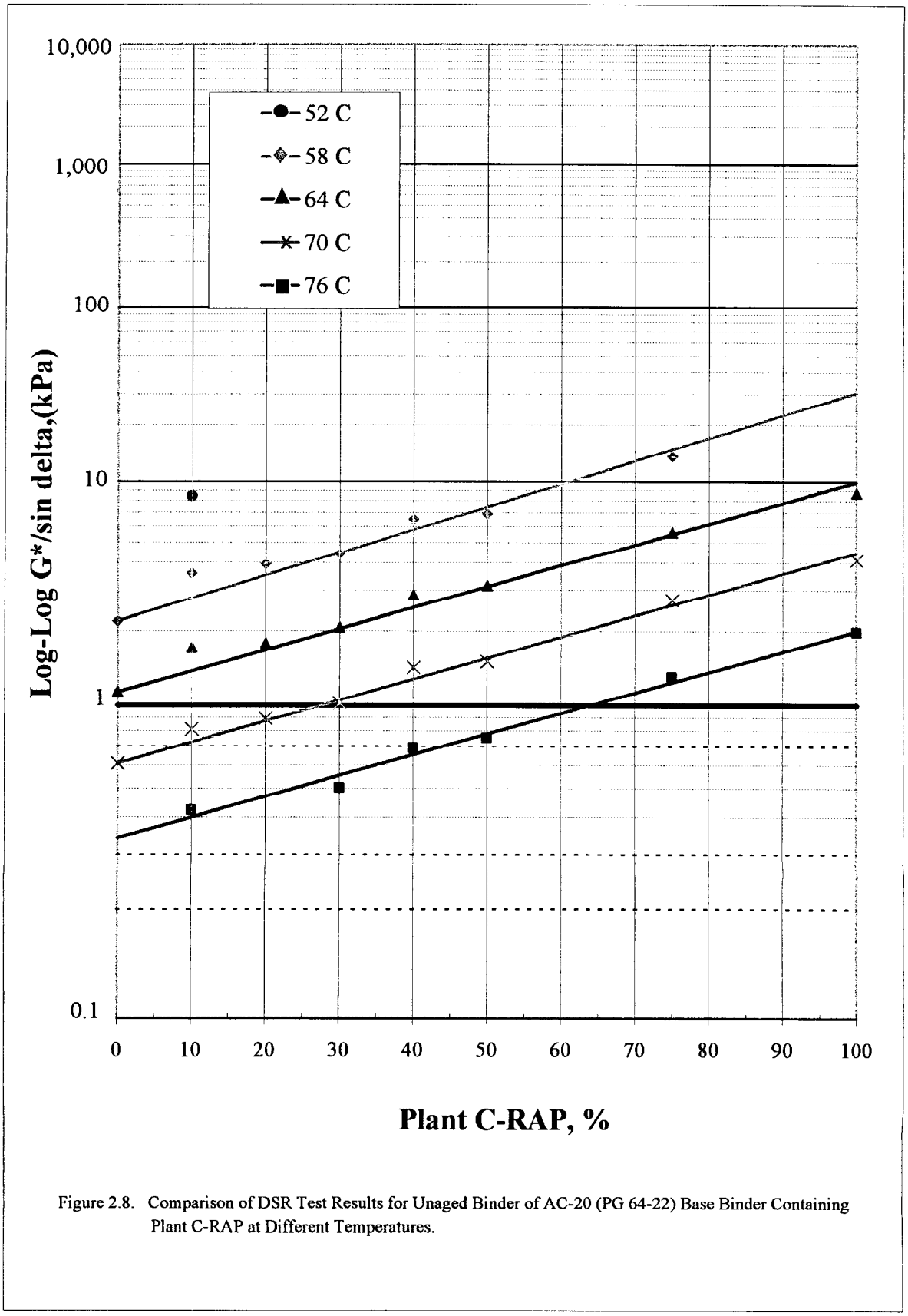

Figure 2.8. Comparison of DSR Test Results for Unaged Binder of AC-20 (PG 64-22) Base Binder Containing Plant C-RAP at Different Temperatures.

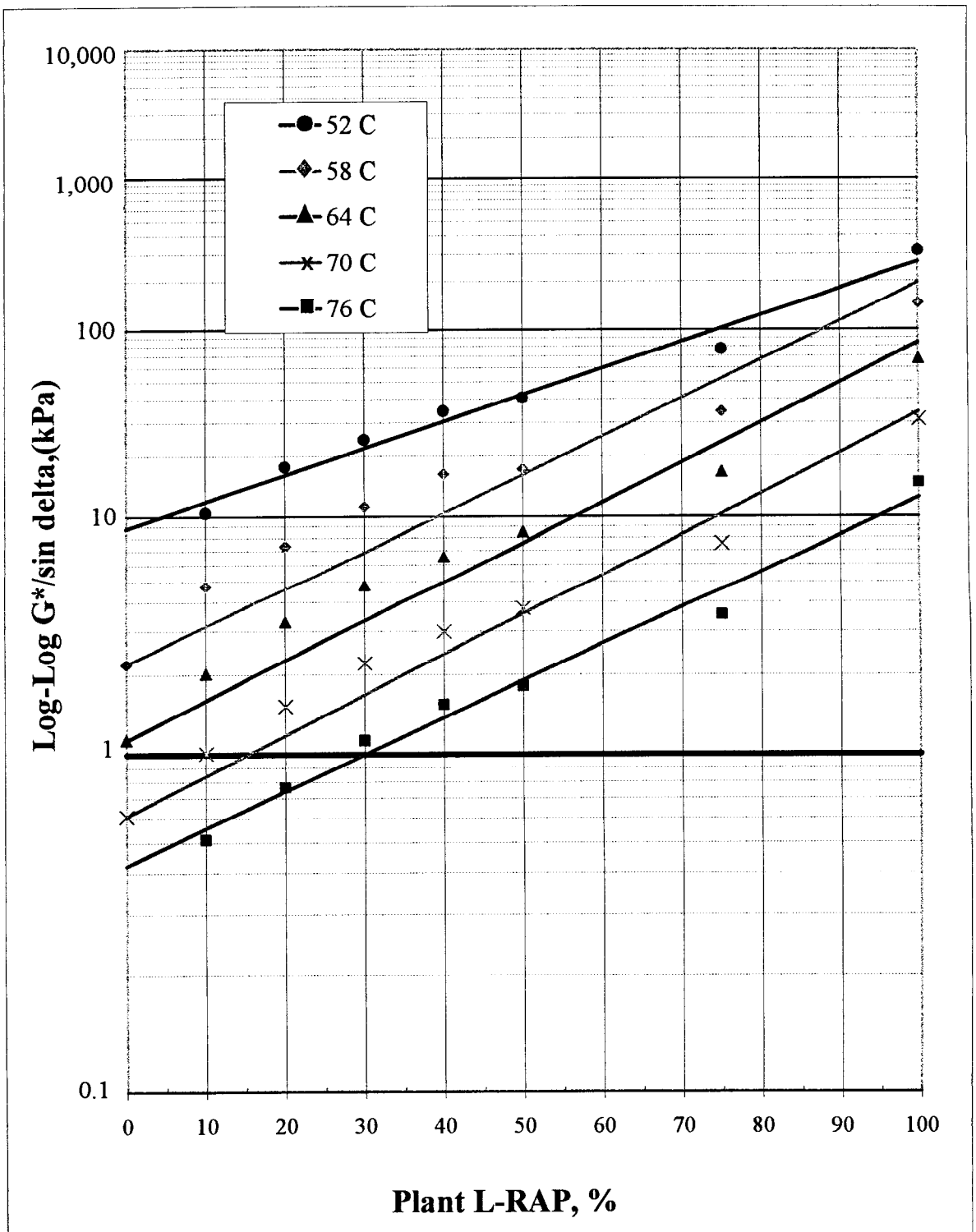

Figure 2.9. Comparison of DSR Test Results for Unaged Binder of AC-20 (PG 64-22) Base Binder Containing Plant L-RAP at Different Temperatures.

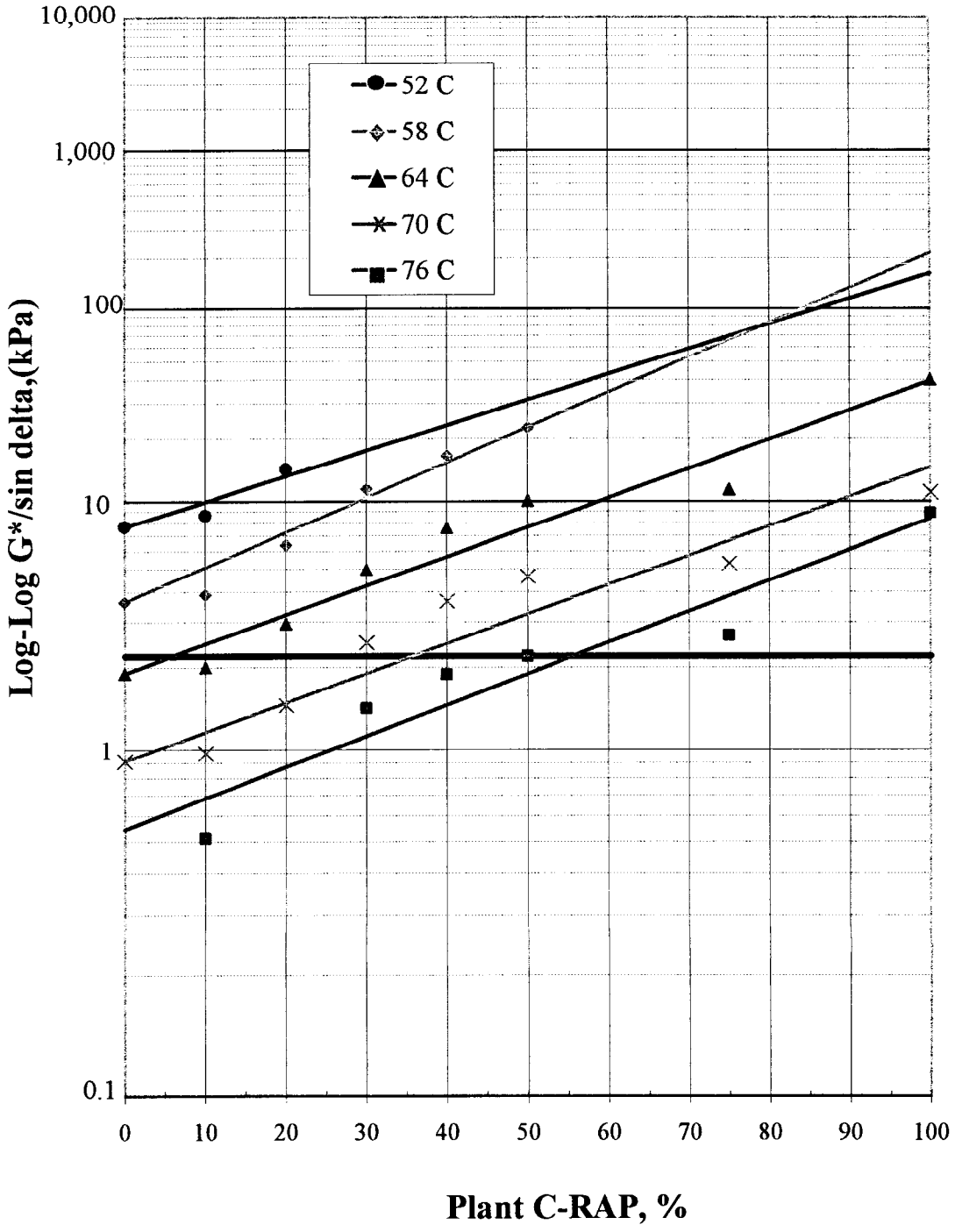

Figure 2.10. Comparison of DSR Test Results for RTFO Aged Binder of AC-10 (PG 58-22) Base Binder Containing Plant C-RAP at Different Temperatures.

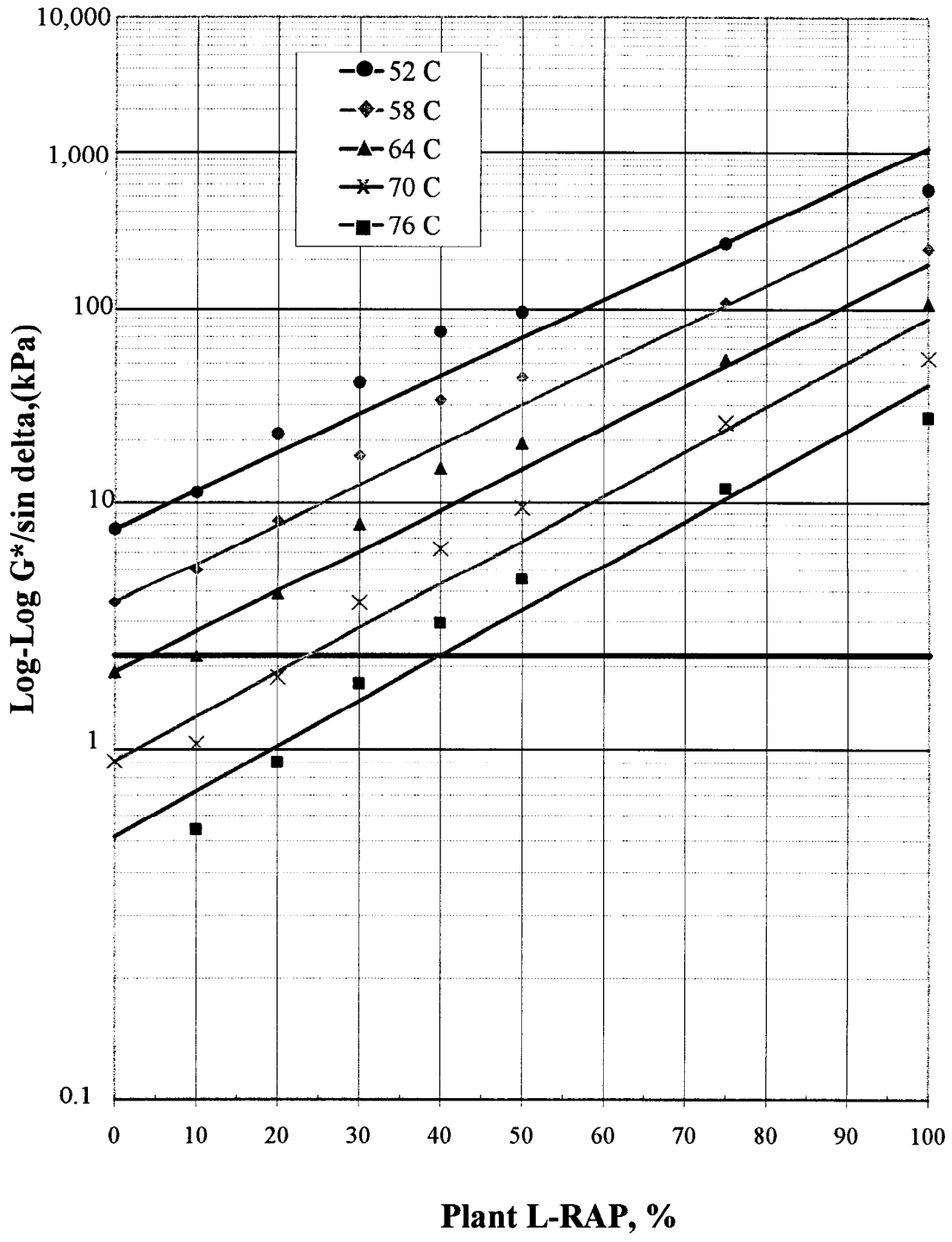

Figure 2.11. Comparison of DSR Test Results for RTFO Aged Binder of AC-10 (PG 58-22) Base Asphalt Containing Plant L-RAP at Different Temperatures.

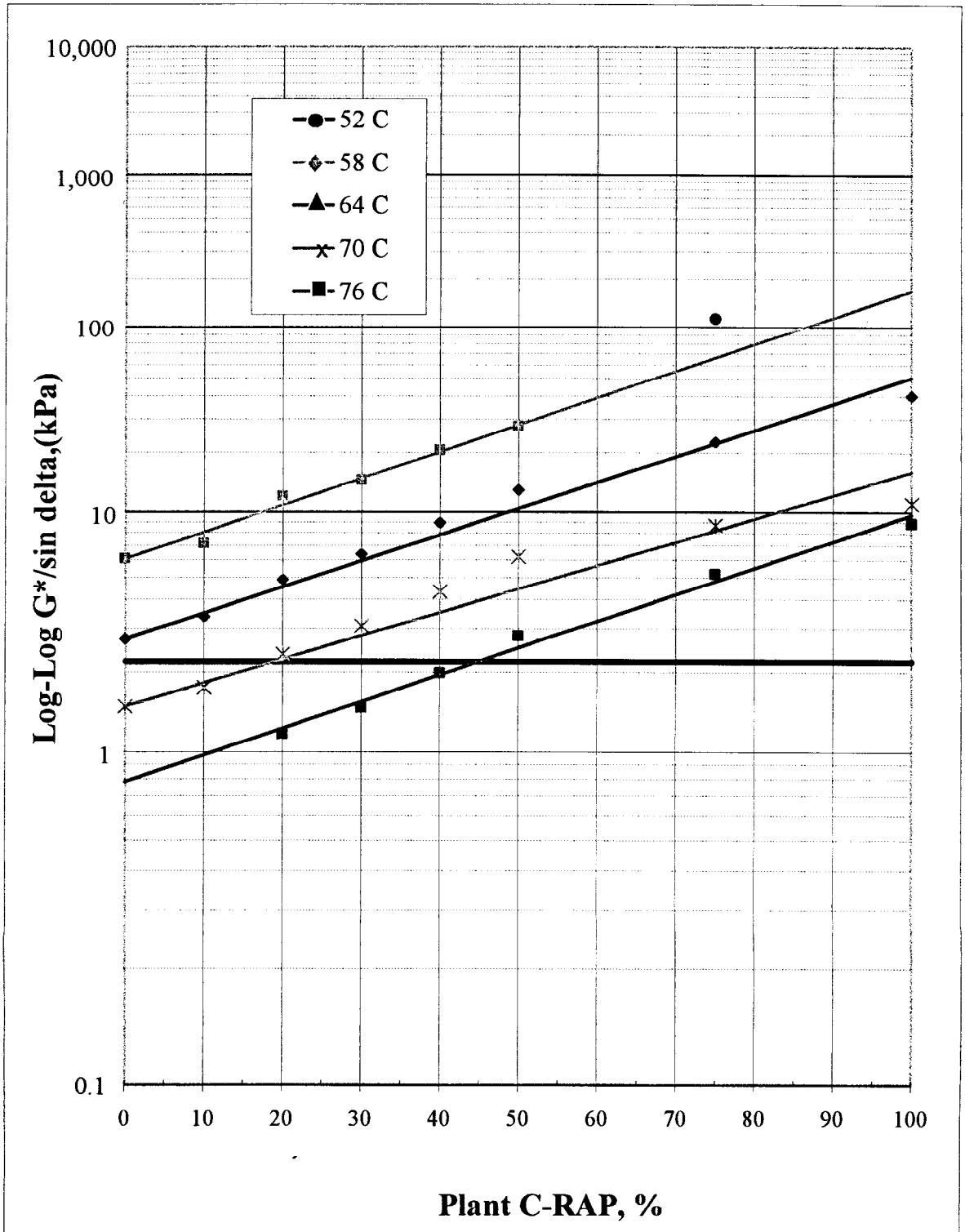

Figure 2.12. Comparison of DSR Test Results for RTFO Aged Binder of AC-20 (PG 64-22) Base Binder Containing Plant C-RAP at Different Temperatures.

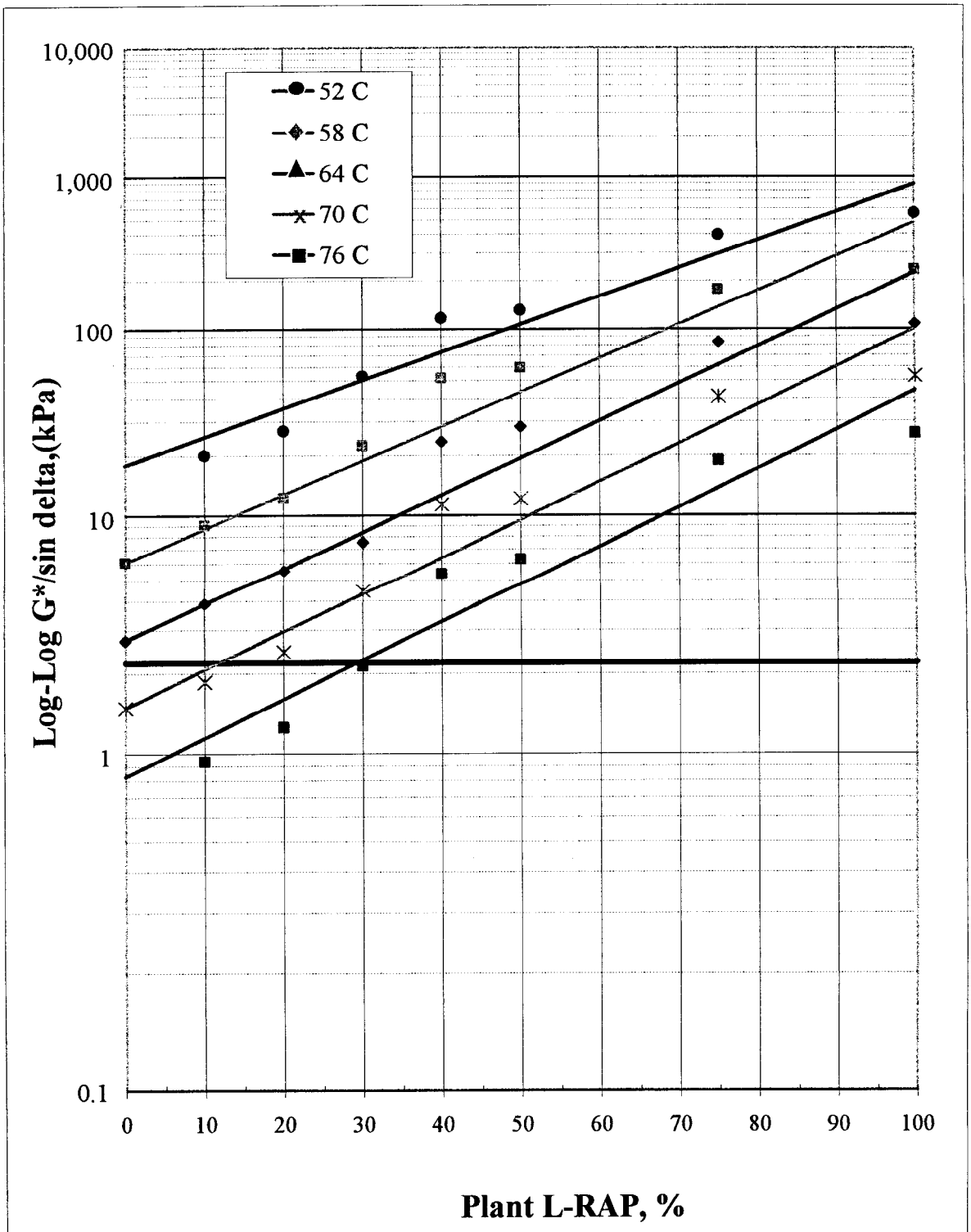

Figure 2.13. Comparison of DSR Test Results for RTFO Aged Binder of AC-20 (PG 64-22) Base Binder Containing Plant L-RAP at Different Temperatures.

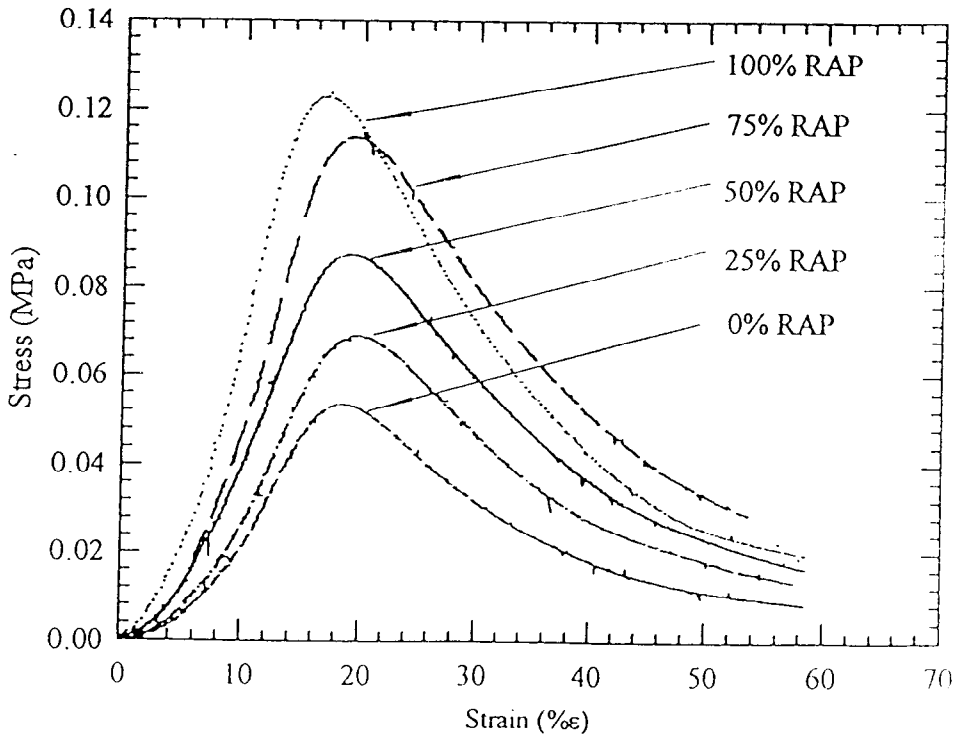

Figure 2.14 Trends in the Quasi-Static Stress-Strain Behavior of RAP.

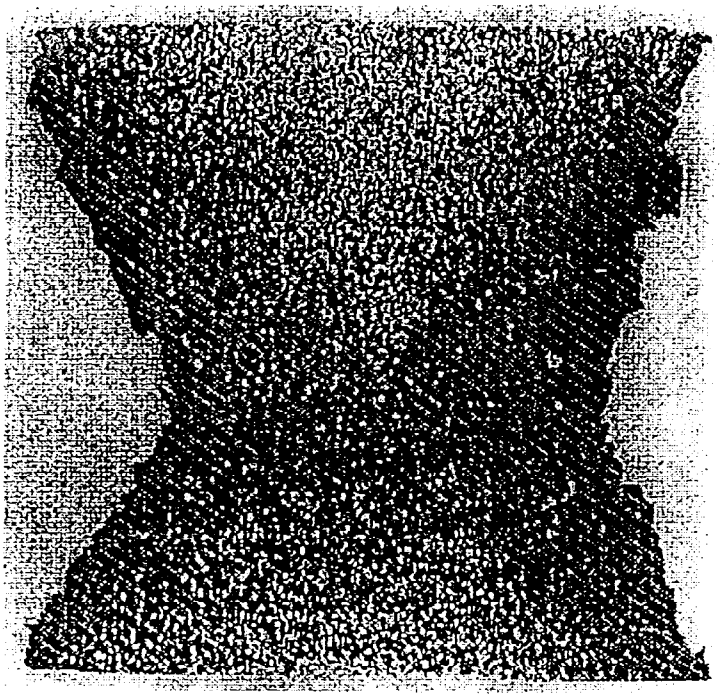

Figure 2.15 Shear Dominance in the 100% RAP Specimen, Typical of all the Specimens Under Loading Condition.

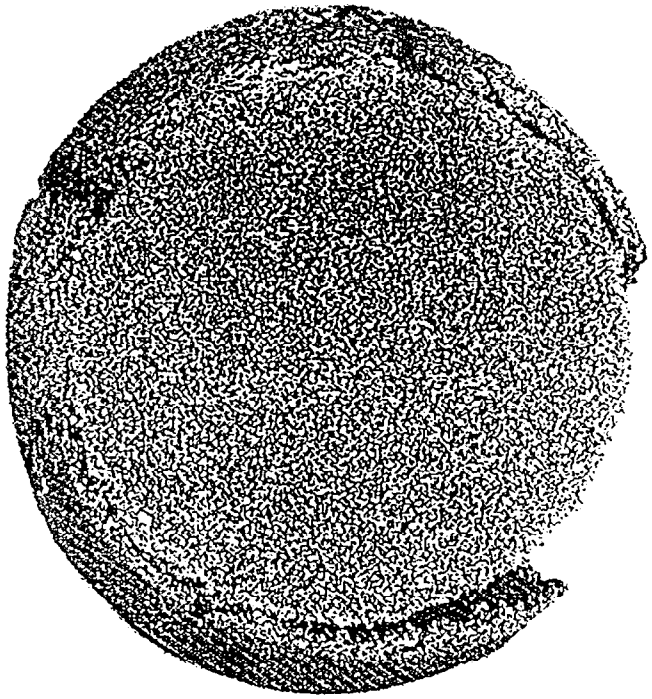

Figure 2.16 Failure of the 100% RAP Specimen, View Shows Circumferential Cracking.

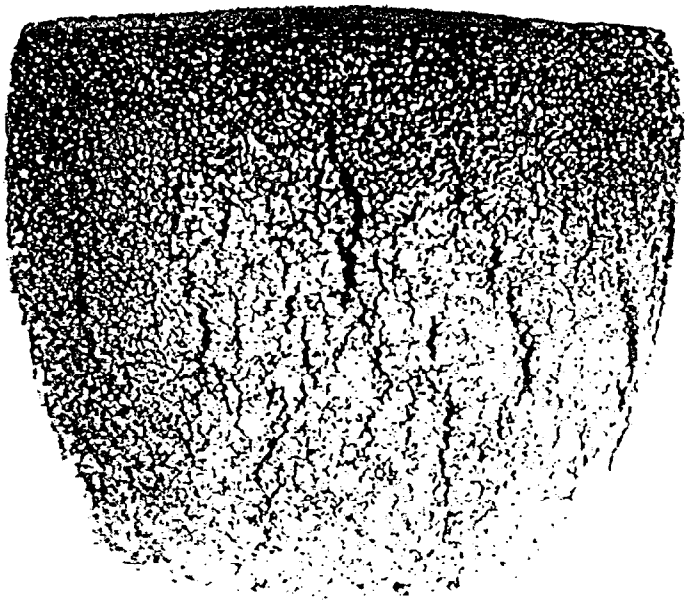

Figure 2.17 Cracking Propagation in the 0% RAP Specimen – Quasi-Static Loading Condition.

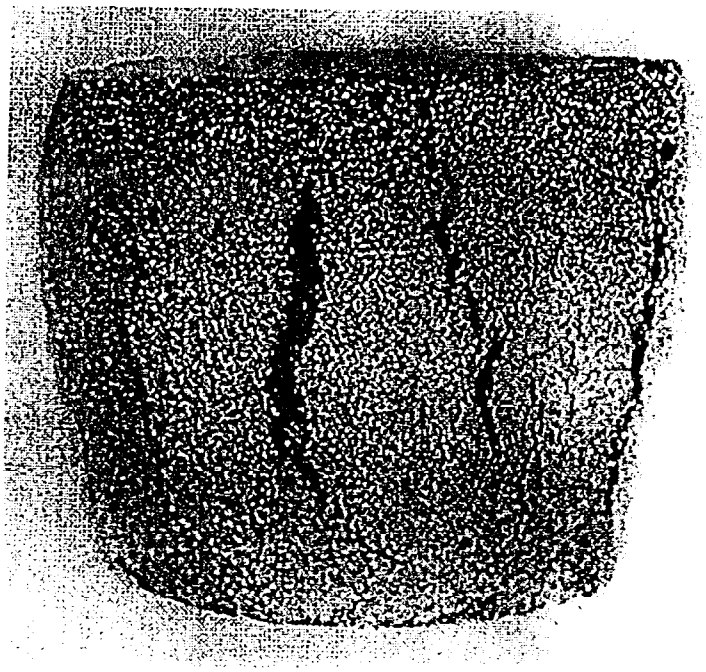

Figure 2.18 Cracking Propagation in the 50% RAP Specimen – Quasi-Static Loading Condition.

3 FATIGUE CRACKING

Fatigue cracking is the phenomenon of fracture under repeated or fluctuating stress lower than the tensile strength in the asphalt mixture. The intermittent longitudinal cracks are the early sign of the fatigue cracking, which usually occurs in the wheel path. Furthermore, the cracks will join and cause more cracks to form. The intermediate stage of fatigue cracking is called "alligator cracking", characterized by transverse cracks connecting the longitudinal cracks. In the severe case, the pothole forms when the aggregates and asphalt binder are no longer bonding. Generally speaking, hot mix asphalt (HMA) must have enough tensile strength to withstand the applied tensile stress at the bottom of the asphalt layer, and be resilient enough to withstand repeated load applications without cracking.

3.1 Rheological Properties and Dynamic Shear Rheometer (DSR)

3.1.1 *Experimental Plan*

Fatigue cracking typically occurs at normal service temperature about 7 to 10 years after pavement construction. The pressure aging vessel (PAV) was used to simulate the long-term aging process of asphalt binder by means of pressurized air and elevated temperature. Pressure of 2.10 MPa is applied to age the RTFO residue at a temperature of 100°C for 20 hours. Then, the DSR tests were performed on the aged binders to evaluate the fatigue cracking resisting characteristics of asphalt binder with RAP at 19, 22, 25, 28 and 31°C. The PAV aged binder is tested at intermediate temperatures to determine the fatigue cracking parameter, $G^*\sin\delta$.

3.1.2 *Test Results and Analysis*

Tables 3.1 and 3.2 summarize the results of DSR tests at different temperatures on the PAV aged binders containing Plant C and L RAPs, respectively.

The maximum limit for the fatigue resistance factor, G*sinδ has been set at 5,000 kPa on RTFO and PAV aged binders. Figures 3.1 and 3.2 show G*sinδ values in a log-log scale on Y-axis at different temperatures versus the RAP contents for PAV residue of AC-10 (PG 58-22) base binders. Figures 3.3 and 3.4 show these values for AC-20 (PG 64-22) base binders. The smaller the G*sinδ value, the more elastic the material and the better resistance to fatigue cracking. From Figures 3.1 and 3.2, it can be seen that G*sinδ was increased as the amount of RAP content increases. The increase in the G*sinδ value is mainly due to G*. Values of δ decreased as the amount of RAP content increases, but did not influence the values of G*sinδ significantly (Tables 3.1 and 3.2). It may be noted that the AC-10 (PG 58-22) base binder containing 55% of Plant C RAP binder content at 22°C or lower temperature in Figure 3.1 did not meet the fatigue resistance criteria. Similarly, it can be observed that the AC-20 (PG 64-22) base binder containing 55% or higher of Plant C RAP did not meet the Superpave binder specification requirement at 25°C, and also the ones with 45% or higher of Plant L RAP did not meet the Superpave binder specification at 25°C as shown in Figure 3.3 and 3.4.

Table 3.3 shows the linear regression models and the R^2 values of base binders containing Plant C and L RAPs. It may be noted that for dynamic shear the calculation gives 1,000 times the tabulated values. It was observed that all R^2 values for Plant C-RAP were observed to be 0.90. This indicated the good linear relationship between the stiffness and RAP content. Some of the R^2 values for Plant L-RAP were observed to be 0.65. It may

be noted that all of the y-intercept in the linear regression models reported in Table 3.3 were set on the stiffness at 0% RAPs. Therefore, the R^2 values decreased for these analyses.

3.2 Fracture Toughness Characterization

Fracture toughness is the value of the stress intensity at which the crack begins to propagate. Early studies on the behavior and performance of bituminous concrete go back to the work of Monismith et al. (1972). The analysis of the experimental results indicated the variation of fracture toughness with asphalt content and consistency as well. The influence of asphalt content on the fracture toughness was found to be dependent upon the test temperature. The concepts of fracture mechanics and fatigue crack growth have considered the effect of various mixture constituents, such as asphalt cement, filler, polymeric and fibrous additives (Majidzadeh et al. 1976). The stress rate dependency of asphaltic overlays was investigated and the fracture toughness was evaluated at various geometrical and loading conditions. The continuously changing stress distribution during the crack growth process is described by linear elastic fracture mechanics principles using Paris' law (Jacobs et al. 1996). Fatigue life was found to be increased as the magnitude of load decreases. A fracture toughness test was used to measure the resistance of a material to crack growth in the present study.

Comprehensive research on the assessment of the performance of a series of asphalt mixes with varying recycled asphalt content was conducted by Sulaiman and Stock (1996). The gradation based on Marshall mix design was implemented in the study. The fracture toughness testing was carried out at three different sub-zero temperatures using the three point beam specimen. Test results indicated the fracture toughness, K_{IC} values at -5°C were

greater than at -15°C but less than those obtained at +5°C. The fracture toughness of a mix containing 70% RAP was found to be marginally higher than values obtained for mixes containing pure binder. However, it was also found that K_{IC} reached a maximum value between +5°C and -15°C for the mix tested. A factor known as the elastic-plastic region, was used to study the elastic-plastic response of the mix. Curiously, the results indicated that the resistance to crack growth was greater at lower temperatures. Also, data showed that RAP content did not have any significant effect on crack growth behavior for the range of mix tested.

3.2.1 *ASTM Fracture Toughness Criteria*

A fracture toughness test essentially measures the resistance of a material to crack extension. Fracture toughness is that value of the stress intensity at which the crack begins to propagate, catastrophically. The present study utilized the procedure of ASTM E399 "Standard Test Method for Plane-Strain Fracture Toughness of Metallic Materials" (ASTM 1996). The standard disk-shaped compact, DC(T), specimen geometry was adopted, mainly because of ease in fabrication. The standard proportions of this geometry are shown in Figure 3.5. The fracture toughness of a material having such a geometry is given by following relation:

$$K_{IC} = \left(\frac{P_{MAX}}{BW^{1/2}} \right) f(a/W) \qquad (1)$$

Where,

K_{IC} = Fracture Toughness, MPa$\sqrt{m}$

P_{max} = Maximum load to failure, N

B = Thickness of the specimen, m

W = Width of the specimen, m

f(a/W) = a factor dependent upon the geometry

$$f(a/W)=\left[\frac{(2+a/W)(0.76+4.8a/W-11.58(a/W)^2+11.43(a/W)^3-4.08(a/W)^4)}{(1-a/W)^{3/2}}\right] \quad (1a)$$

The blank specimen had a diameter of 101.6 mm, and had a width of 76.2 mm (D = 1.35W). The thickness of the specimen was 38.1 mm, as per the relation W/B = 2. For an initial crack length of 34.29 mm, and an a/W ratio of 0.45, the f(a/W) factor was calculated as 8.71.

3.2.2 *Fracture Toughness Characterization Experiments*

The asphalt cement and Plant C RAP binder were heated to 160°C for an hour, till they started to flow. They were further mixed with 550 grams of heated aggregates. The weight of binder as a percentage of the total weight was established by performing preliminary tests and the maximum value of fracture toughness was found to occur at 6% binder content. This mixture was then compacted with 55 blows on either face to account for proper compaction. Finally, the specimen was ejected, cured overnight and machined to the required dimensions. The edge crack was band-sawed and was sharpened up to 1 mm using a diamond saw to provide a sharp crack. The Instron testing machine was used to load the specimen. It was made sure that the loading pins were sufficiently lubricated so as to nullify frictional effects.

3.2.3 *Rate Dependency of Virgin Asphalt Binder*

In order to study the rate dependency of the virgin asphalt binder, experiments were carried out to evaluate K_{IC} at different rates of loading from 25.4 mm per minute all the way up to 254 mm per minute. The results from this study are shown in Figure 3.6. As can be seen from the figure, a gradual increase in fracture toughness was noticed with an increasing rate. However, the values stabilized for rates over 152.4 mm per minute. Thus it was decided that further experimentation would be carried out at a displacement rate of 152.4 mm/minute. The maximum average fracture toughness obtained for the virgin binder was 78 MPa$\sqrt{m}$. The error generated in data was within a band of ±10 % and well within tolerable experimental consistencies.

3.2.4 *Room Temperature Experiments - K_{IC} Evaluation*

After determining the rate of loading to be used, further experimentation was carried out in a two phase manner. Firstly, the fracture behavior of binders with RAP was studied at room temperature, in order to evaluate fatigue cracking resistance. Secondly, the low temperature fracture characterization was conducted to examine the brittle fast failure, i.e., low-temperature cracking in the upper layers of the pavement.

Two specimens were tested at each increment of 25% RAP content and at the loading rate of 152.4 mm per minute. Also crack sharpening was consistently maintained in all the cases so as to obtain an accurate estimate of fracture toughness.

The trends from the experiments can be represented by a quadratic curve fit as shown in Figure 3.7. The percentage increase in the fracture toughness values for the 25%

and 50% RAP cases were 5% and 6.3 %, respectively when compared to the 0% RAP case. However, there was a significant increase of 71% in the toughness values when 75% RAP was added to the virgin binder. The maximum increase of 118% was noticed in the case of the 100% RAP specimen.

In order to understand this behavior better, the crack propagation in all the specimens was studied. The crack propagation for the 0%, 50% and 100% RAP specimen are shown in Figures 3.8 through 3.10, respectively. A most common feature as shown by the photographs is the stable crack propagation leading to final arrest. Also the cracks seem to have propagated in an irregular manner. By a more careful observation of the 0% RAP specimen, it can be seen that the crack actually branched through a distance of 15.24 mm before finally arresting. The crack jump distance increased as the RAP content increased, and is perhaps indicative of reduced arrest toughness. Although stable crack growth was observed in all the experiments, the crack tended to propagate unstably in the 100% RAP specimen. Also the crack opening displacement seems to have decreased with RAP content. These visual observations are indications of plastic zones ahead of the crack front. In this vein it can be concluded that the addition of RAP is decreasing the ductility inherent in the binder and causing it become rather brittle.

3.3 Dynamic Characterization Using the Split Hopkinson Pressure Bar (SHPB)

The dynamic response of asphalt to compressive stress pulses induced due to traffic loads plays a significant role in the flexible pavement structures. The dynamic response of various asphalt mixtures and over range of frequencies were studied by Majidzadeh et al. (1976). The dynamic modulus, E* was found to be dependent on the nature and percentage

of additives used. The most effective additives were found to be sulfur, petroset emulsion and asbestos fiber. Also the dynamic modulus was found to decrease with increase in temperature indicating plasticity effects. Sousa and Monismith (1988) idealized the pavement as a multi-layer elastic or viscoelastic system, i.e., the system response to dynamic loads were assumed to have internal damping and hence a phase lag 'd'. Test results indicated that the stiffness-modulus strongly depended on frequency and temperature. The internal damping was found to decrease with the increasing frequency and temperature. Strangely, the dynamic modulus was found to be independent of the stress level for the range of frequencies employed. Both the dynamic modulus and the shear modulus were found to be dependent on the density of the specimen. Also Poisson's ratio was found to decrease with increasing frequency of loading.

Sulaiman and Stock (1996) conducted experiments to determine the dynamic stiffness of asphalt mixes with varying percentages of reclaimed asphalt. Testing was conducted over a range of temperatures and frequencies of sinusoidal loads. It was observed that the maximum stability was achieved with a mixture having 70% RAP by weight. However, it was also shown that incorporating RAP made a significant difference to the dynamic stiffness of the mix. At higher temperature, E* was decreased.

3.3.1 *The SHPB for High Strain Rate Compression Testing*

The SHPB was used to study the dynamic behavior in the present study. The SHPB technique is a well established experimental technique used to study dynamic behavior in both ductile and brittle materials alike (Lindholm and Yeakley 1968; Davies and Hunter 1963; Nemat-Nasser et al. 1991; Malvern and Ross 1985). A conventional SHPB or the

Kolsky Bar consists of a striker bar, an incident bar and a transmitter bar, as illustrated in Figure 3.11 (Kolsky 1949). The specimen under study is sandwiched between the incident and transmitter bar. The striker bar is launched at a predefined velocity towards the incident bar. This impact generates a compressive stress pulse, which travels towards the specimen. The amplitude of the stress pulse is a function of the velocity of the striker bar, and its period is approximately equal to twice the travel time of the wave in the striker bar. This wave, upon reaching the incident bar-specimen interface, gets partly reflected back and partly transmitted into the specimen depending on the impedance mismatch and the area mismatch between the specimen and the bar. From one-dimensional wave theory, it has been established that the amplitude of the transmitted pulse is a measure of the stress in the specimen and the amplitude of the reflected pulse is a measure of the strain rate in the specimen. Thus upon integrating the reflected pulse, the strain in the specimen can be determined. The specimen can be subjected to a wide range of strain rates by employing striker bars of various lengths.

3.3.2 *Governing Equations*

The fundamental relations stem from the classical D'Alembert-one dimensional wave equation given by

$$\mu(x,t) = f(x - c_0 t) + g(x + c_0 t) \tag{2}$$

where 'f' and 'g' represent propagating disturbances and are arbitrary functions of integration determined by the initial conditions of the forcing function of a given problem. Also, 'f' corresponds to a wave traveling in the positive x direction and 'g' corresponds to a wave traveling in the negative x-direction. A schematic of the incident, reflected and the transmitted strain pulses, ε_i, ε_r, and ε_t are provided in Figure 3.12. From one dimensional

rod theory, the displacements at the two specimen-bar interfaces are given by

$$\mu_1 = c_0 \int_0^t (-\varepsilon_i + \varepsilon_r)dt \tag{3}$$

$$\mu_2 = -c_0 \int_0^t (\varepsilon_t)dt \tag{4}$$

The average strain of the specimen, ε_s, is then given by,

$$\varepsilon_s = \frac{c_0}{l_s} \int_0^t (\varepsilon_i - \varepsilon_r - \varepsilon_t)dt \tag{5}$$

where 'l_s' is the original length of the specimen. The loads at the two interfaces are given by,

$$P_1 = A_b E_b (\varepsilon_i + \varepsilon_r) \tag{6}$$

$$P_2 = A_b E_b \varepsilon_t \tag{7}$$

where, 'A_b' is the cross-sectional area of the bars. Now, an important assumption is made that wave propagation effects within short specimen may be neglected, thus $P_1 = P_2$. From this, it follows that $\varepsilon_i + \varepsilon_r = \varepsilon_t$, and so, equation (5) simplifies to

$$\varepsilon_s(t) = \frac{-2c_0}{l_s} \int_0^t (\varepsilon_r)dt \tag{8}$$

The average stress in the specimen is given by,

$$\sigma_s = E_b \left(\frac{A_b}{A_s} \right) \varepsilon_t \qquad (9)$$

where, 'E_b' is the modulus of elasticity of the pressure bars, 'A_s' is the instantaneous cross sectional area of the specimen and 'c_o', the wave speed in the bar, is known to be $\sqrt{(E/\rho)}$, 'ρ' being the mass density of the bar material.

There are following two fundamental assumptions in deriving the above equations. Firstly, wave propagation within the pressure bars must remain one-dimensional. Since the strain gages measure surface displacements, it is extremely important that this condition is met. This essentially means that the wave can be assumed to be one-dimensional and surface displacements are accurate indicators of surface axial displacements in the bars. Secondly, the specimen must undergo homogenous deformation. Uniform deformation is generally hindered by radial and longitudinal inertia of the specimen and the frictional contact at the specimen-bar interfaces. Hence, it is customary to use oil-based molybdenum disulfide as a lubricant for experiments conducted at room temperature.

3.3.3 *Dynamic Characterization Experiments*

The dynamic characterization experiments were conducted by fabricating specimens having a diameter of 43.2 mm (1.729 in.) and a length of 0.125 mm (0.5 in.). The diameter was selected so as to provide a cross-sectional area mismatch between the pressure bars (diameter 50 mm) and the specimen of 25%, assuming a maximum strain of 25% in the specimen. This ensured that the specimen diameter did not exceed the diameter of the bars

as it expanded radially.

The weight of aggregates needed for specimen fabrication was obtained from volume considerations, i.e., by linearly scaling down the volume needed for fabricating the DC(T) specimen for fracture toughness testing. Accordingly, the weight of aggregates came down to 35 grams. The specimen constituents were the same as the ones in fracture toughness testing and the specimen was compacted in accordance with the procedure of Kennedy et al. (1982).

3.3.4 *Dynamic Response of Virgin Asphalt and RAP Binder at Room Temperature*

Experiments were conducted to determine the dynamic response of virgin and RAP binders. The dynamic flow stress was evaluated at every increment in RAP content and at room temperature (~22°C). The SHPB system in conjunction with the high speed data acquisition system, LECROY, was used for this study and a user-defined code was compiled to aid in data manipulation. All the experiments were carried out at a nominal strain rate of 450 /s in order to establish a base for performance comparison.

The typical strain pulses obtained in these set of experiments are indicated in Figure 3.13. The nominal wave speed in asphalt, was estimated to be 211 m/s. A typical plot of the strain history is provided in Figure 3.14. The trends in the true stress-strain response from 0° and 22°C experiments are provided in Figure 3.15. Also the variation of dynamic flow stress as a function of RAP content is provided in Table 3.4 and the trends are presented in Figure 3.16. As can be perceived, the flow stress increased as the percentage of RAP was increased. There was a nominal increase of 6% in the values of flow stress obtained for the 25% and 50% RAP specimen when compared to flow stress of 0% RAP. An increase of

12% in the flow stress values was noticed for the 75% RAP specimen. The largest increment of 26% was noticed in the case of the 100% RAP specimen.

The specimen failure was noticed to be shear dominated, much like the one observed in the quasi-static experiments. An examination of the specimen face (facing the incident bar) revealed the presence of circumferential cracks, radial cracks and longitudinal cracks as shown in Figure 3.17 (75% RAP specimen). A more predominant segment formation was noticed in these specimens as compared to specimens tested under static loading conditions. It seems quiet possible that cracking initiated because of circumferential stresses along the periphery of the specimen. As previously mentioned, these stresses may have been caused due to inertial and frictional effects. These reasons may also have been a factor leading to the formation of larger wedge shapes. The side view of the 75% RAP specimen, Figure 3.18, indicates the shear dominant failure in the specimen. This type of failure was typical of all the specimen that failed at room temperature. These visual observations and trends from the dynamic true stress-strain plots are indicators of reduced ductility in the specimen as the RAP percentage increased. The observations from the quasi-static experiments accentuate this argument.

Table 3.1 DSR Test Results of PAV aged Asphalt Binders Containing Plant C-RAP.

RAP, %	Temps, C	PAV Aged					
		AC 10			AC 20		
		G*	δ	G*sinδ	G*	δ	G*sinδ
0	19	5604	45.6	4004	8587	43.1	5867
	22	3616	49.0	2729	5601	46.1	4036
	25	2210	52.8	1760	3572	49.5	2716
	28	1489	55.2	1223	2232	52.6	1773
	31	910	58.5	776	1348	56.4	1123
10	19	6654	43.7	4597	8480	45.0	5996
	22	4314	46.8	3145	5726	48.0	4255
	25	2777	49.7	2118	3801	49.5	2890
	28	1749	52.9	1395	2516	52.1	1985
	31	1072	56.2	891	1528	55.2	1255
20	19	8067	41.1	5303	9493	40.6	6178
	22	5340	43.8	3696	6395	43.2	4378
	25	3472	46.8	2531	4098	46.3	2963
	28	2195	49.9	1679	2650	49.3	2009
	31	1348	53.2	1079	1687	52.3	1335
30	19	9362	38.8	5866	10594	39.0	6667
	22	6303	41.6	4185	7181	42.0	4805
	25	4186	44.2	2918	4790	45.0	3387
	28	2748	47.2	2016	3151	47.9	2338
	31	1751	50.5	1351	2013	51.2	1569
40	19	10817	36.5	6434	13283	37.0	7994
	22	7492	39.1	4725	9219	39.8	5901
	25	5089	41.5	3372	6218	42.4	4193
	28	3412	44.2	2379	4166	45.3	2961
	31	2195	47.6	1621	2629	48.7	1975
50	19	11224	36.2	6629	13591	38.1	8386
	22	7793	38.5	4851	10697	39.2	6761
	25	5356	41.3	3535	7318	41.9	4887
	28	3630	43.6	2503	4895	44.7	3443
	31	2368	47.1	1735	3186	47.9	2364
75	19	14450	33.1	7891	16323	33.7	9057
	22	10267	35.2	5918	12576	35.6	7321
	25	7167	37.6	4373	9452	38.3	5858
	28	6376	39.6	4064	6479	40.9	4242
	31	4221	42.8	2868	4285	43.9	2971
100	19	19206	31.3	9978	19206	31.3	9978
	22	13907	33.5	7676	13907	33.5	7676
	25	11885	35.2	6851	11885	35.2	6851
	28	6939	38.4	4310	6939	38.4	4310
	31	4752	41.5	3149	4752	41.5	3149

Table 3.2 DSR Test Results of PAV aged Asphalt Binders Containing Plant L-RAP.

RAP, %	Temps, C	PAV Aged					
		AC 10			AC 20		
		G*	δ	G*sinδ	G*	δ	G*sinδ
0	19	5604	45.6	4004	8587	43.1	5867
	22	3616	49.0	2729	5601	46.1	4036
	25	2210	52.8	1760	3572	49.5	2716
	28	1489	55.2	1223	2232	52.6	1773
	31	910	58.5	776	1348	56.4	1123
10	19	6805	43.1	4650	10877	40.5	7064
	22	4465	46.2	3223	7297	43.2	4995
	25	2890	49.2	2188	4756	46.4	3444
	28	1838	52.4	1456	3057	49.2	2314
	31	1109	56.0	919	1911	52.5	1516
20	19	10221	38.5	6363	11978	37.7	7325
	22	6923	41.2	4560	8239	40.5	5351
	25	4629	43.9	3210	5548	43.4	3812
	28	3034	46.7	2208	3674	46.0	2643
	31	1919	50.1	1472	2318	49.9	1773
30	19	12187	34.9	6973	13410	36.0	7882
	22	8486	37.1	5119	9228	38.4	5732
	25	5879	39.8	3763	6299	41.2	4149
	28	4031	42.5	2723	4268	44.0	2965
	31	2653	45.5	1892	2775	47.2	2036
40	19	13858	33.1	7568	16987	33.0	9252
	22	9868	35.2	5688	13853	25.5	5964
	25	6921	37.6	4223	7635	38.1	4711
	28	4793	40.1	3087	5725	40.7	3733
	31	3220	42.9	2192	3282	43.5	2259
50	19	15420	31.5	8057	18179	32.2	9687
	22	11037	33.5	6092	13773	34.0	7702
	25	7955	35.6	4631	9868	36.3	5842
	28	6233	37.8	3820	6955	38.8	4358
	31	4273	40.5	2775	4735	41.4	3131
75	19	17660	27.4	8127	20828	28.7	10002
	22	13211	29.2	6445	-9774	305.0	8006
	25	9902	30.9	5085	14475	32.1	7692
	28	7280	33.0	3965	8501	34.5	4815
	31	5180	35.2	2986	6123	37.2	3702
100	19	22931	26.8	10339	22931	26.8	10339
	22	17348	28.1	8171	17348	28.1	8171
	25	15889	29.6	7848	15889	29.6	7848
	28	9716	31.4	5062	9716	31.4	5062
	31	7058	33.6	3906	7058	33.6	3906

Table 3.3 The Linear Regression Models and Coefficient of Determinations (R^2) for Plant C and L RAP.

Dependent Parameter, Y	Temperature, (°C)	AC-10 (PG 58-22)	AC-20 (PG 64-22)
RAP from Plant C			
G*sinδ determined by DSR test for PAV aged binder	19	$Y = 0.8197 + 0.0002708X$ $R^2 = 0.9420$	$Y = 0.8305 + 0.0001574X$ $R^2 = 0.9293$
	22	$Y = 0.8086 + 0.0003143X$ $R^2 = 0.9464$	$Y = 0.8199 + 0.0002087X$ $R^2 = 0.8999$
	25	$Y = 0.7956 + 0.0003990X$ $R^2 = 0.9611$	$Y = 0.8085 + 0.0002786X$ $R^2 = 0.9591$
	28	$Y = 0.7844 + 0.0004263X$ $R^2 = 0.9547$	$Y = 0.7958 + 0.0003060X$ $R^2 = 0.9878$
	31	$Y = 0.7701 + 0.0004835X$ $R^2 = 0.9591$	$Y = 0.7818 + 0.0003584X$ $R^2 = 0.9367$
RAP from Plant L			
G*sinδ determined by DSR test for PAV aged binder	19	$Y = 0.8197 + 0.0003111X$ $R^2 = 0.6789$	$Y = 0.8305 + 0.0002013X$ $R^2 = 0.6528$
	22	$Y = 0.8086 + 0.0003699X$ $R^2 = 0.7189$	$Y = 0.8199 + 0.0002491X$ $R^2 = 0.7441$
	25	$Y = 0.7956 + 0.0004798X$ $R^2 = 0.8145$	$Y = 0.8085 + 0.0003587X$ $R^2 = 0.9026$
	28	$Y = 0.7844 + 0.0005099X$ $R^2 = 0.7633$	$Y = 0.7958 + 0.0003887X$ $R^2 = 0.7571$
	31	$Y = 0.7701 + 0.0005913X$ $R^2 = 0.7897$	$Y = 0.7818 + 0.0004596X$ $R^2 = 0.8255$

Note: Independent variable, X indicates the amount of RAP in asphalt binder.

Table 3.4 Results of Dynamic Characterization of RAP Binder.

(a) Room Temperature

0%RAP		25%RAP		50%RAP		75%RAP		100%RAP	
Flow Stress (MPa) and Flow Strain (%ε) at 22°C									
26	7.8	27	7.5	28	8.2	30	9.2	32	8.5
26	7.5	27	7.5	27	7.5	29	7.8	34	8.5
Average Values of Flow Stress and Flow Strain									
26	7.7	27	7.5	27.5	7.9	29.5	8.5	33	8.5
Strain Rate at 22°C									
456		457		448		462		451	

(b) Low Temperature

0%RAP		25%RAP		50%RAP		75%RAP		100%RAP	
Flow Stress (MPa) and Flow Strain (%ε) at 0°C									
31.5	7.2	34	7	32	7	32	7	34	7
Strain Rate at 0°C									
456		429		433		446		448	

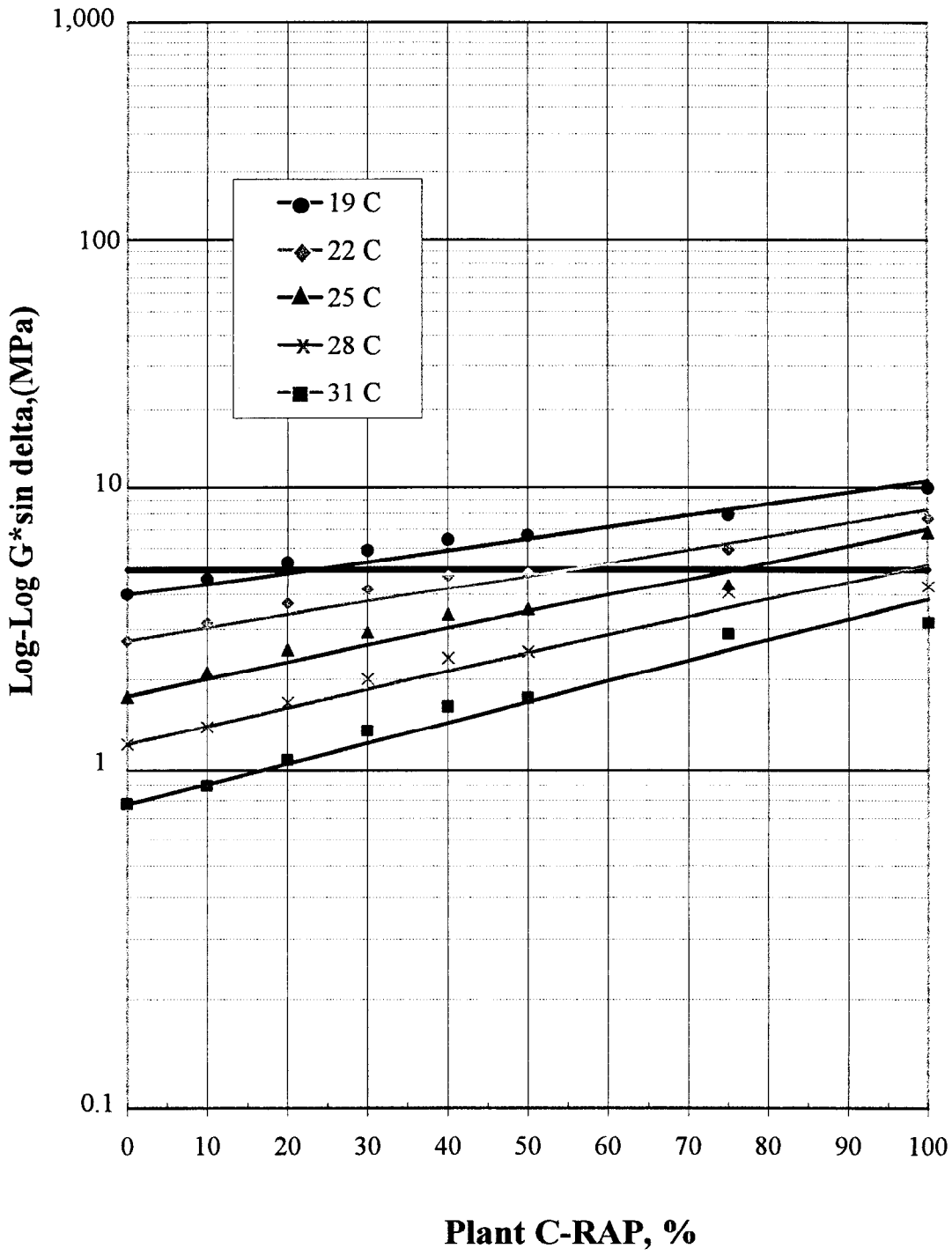

Figure 3.1. Comparison of DSR Test Results for PAV Aged Binder of AC-10 (PG 58-22) Containing Plant C-RAP at Different Temperatures.

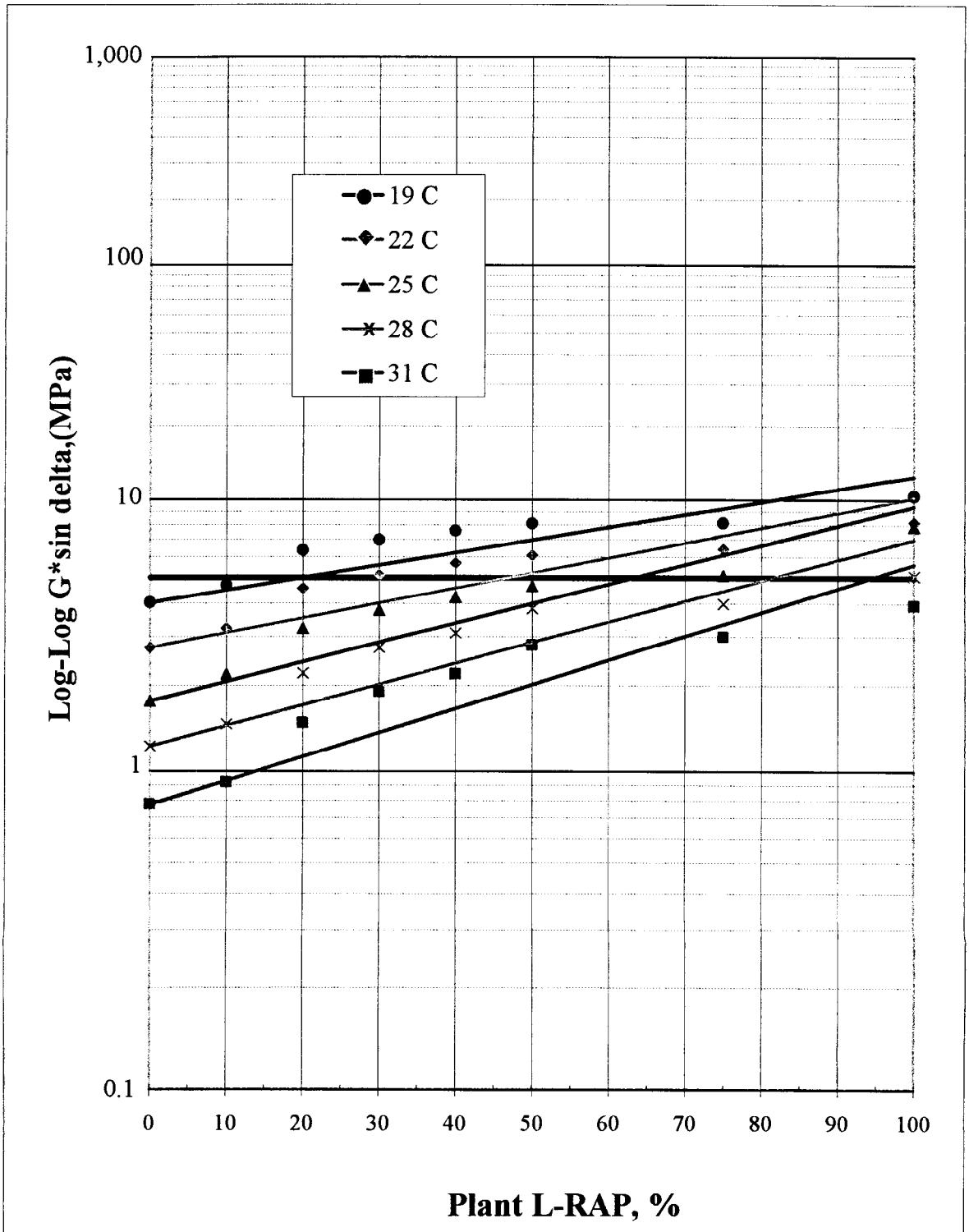

Figure 3.2. Comparison of DSR Test Results for PAV Aged Binder of AC-10 (PG 58-22) Base Asphalt Containing Plant L-RAP at Different Temperatures.

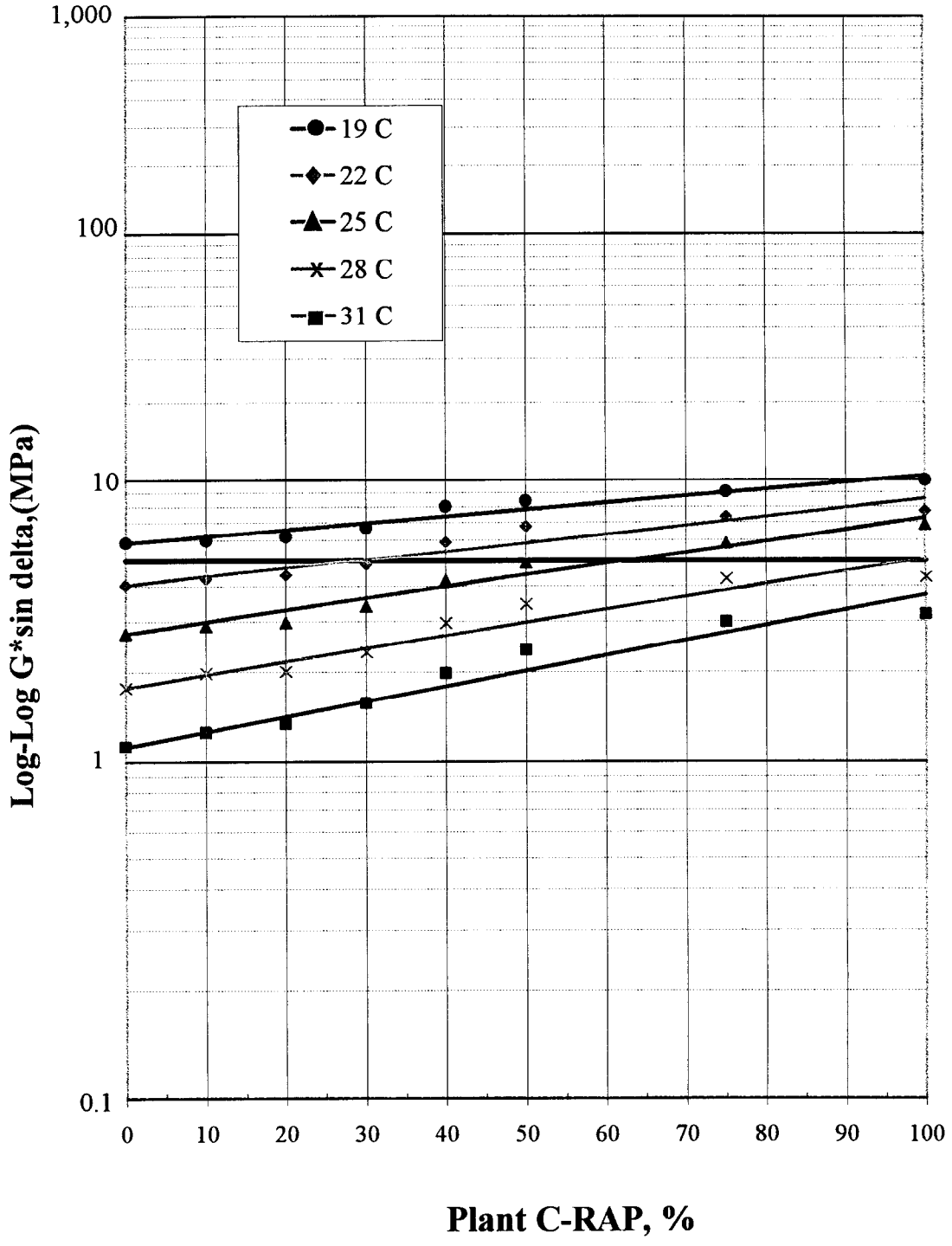

Figure 3.3. Comparison of DSR Test Results for PAV Aged Binder of AC-20 (PG 64-22) Containing Plant C-RAP at Different Temperatures.

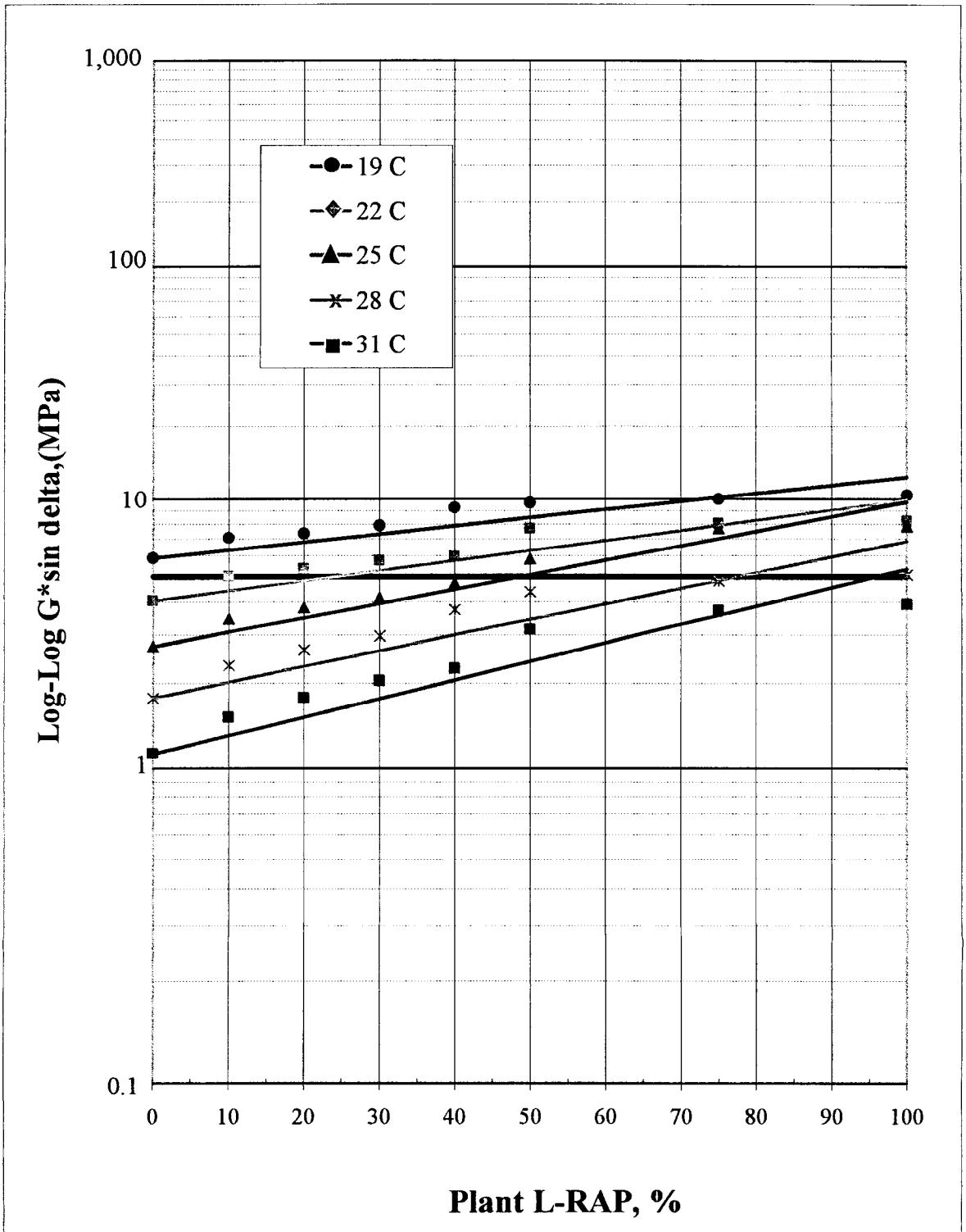

Figure 3.4. Comparison of DSR Test Results for PAV Aged Binder of AC-20 (PG 64-22) Containing Plant L-RAP at Different Temperatures.

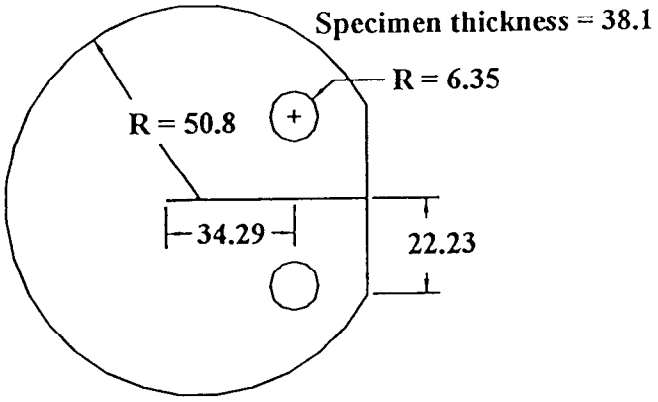

Figure 3.5 Standard Geometry of Disc Shaped Compact Specimen, DC(T).

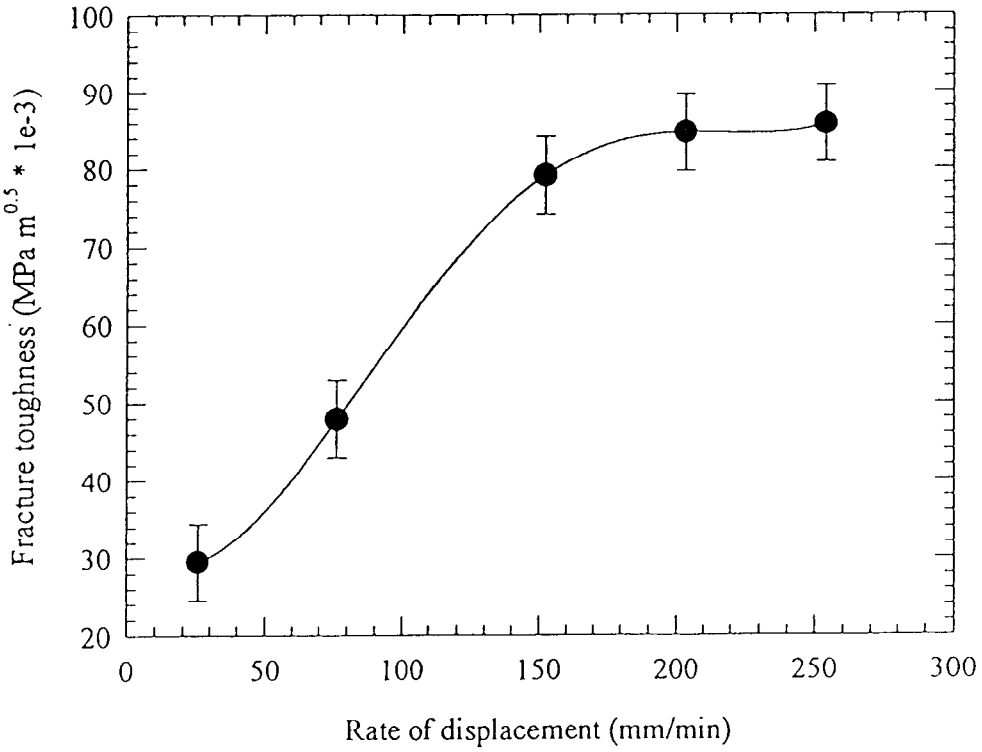

Figure 3.6 Variation of Fracture Toughness with Rate of Loading.

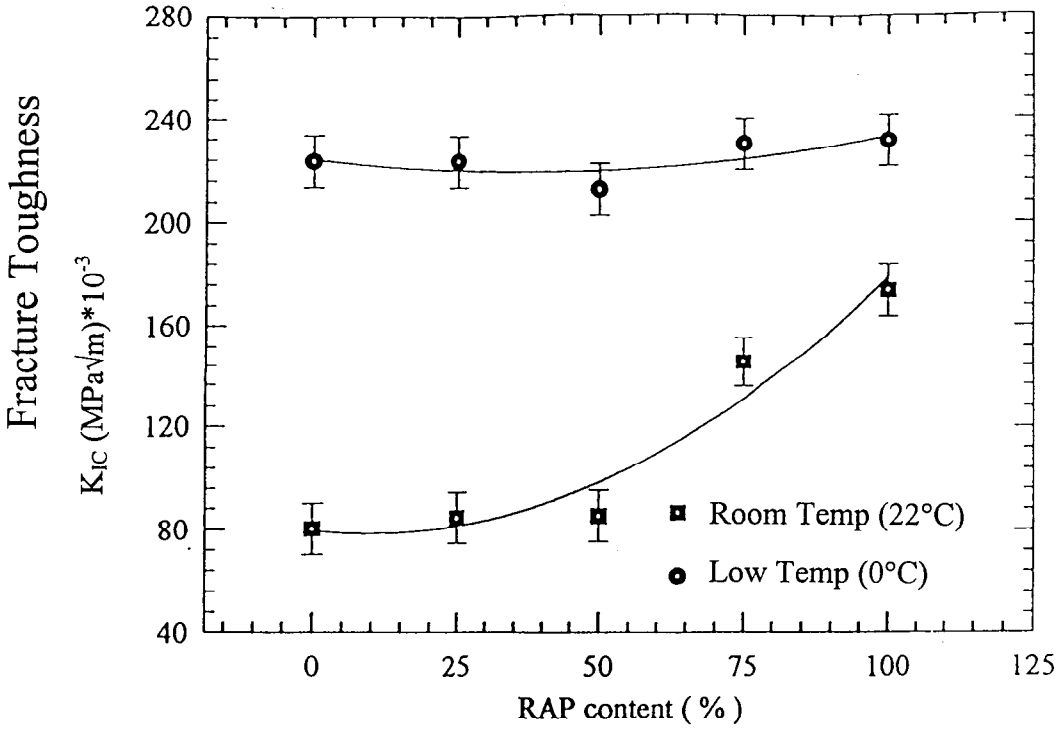

Figure 3.7 Variation of Fracture Toughness with RAP Content.

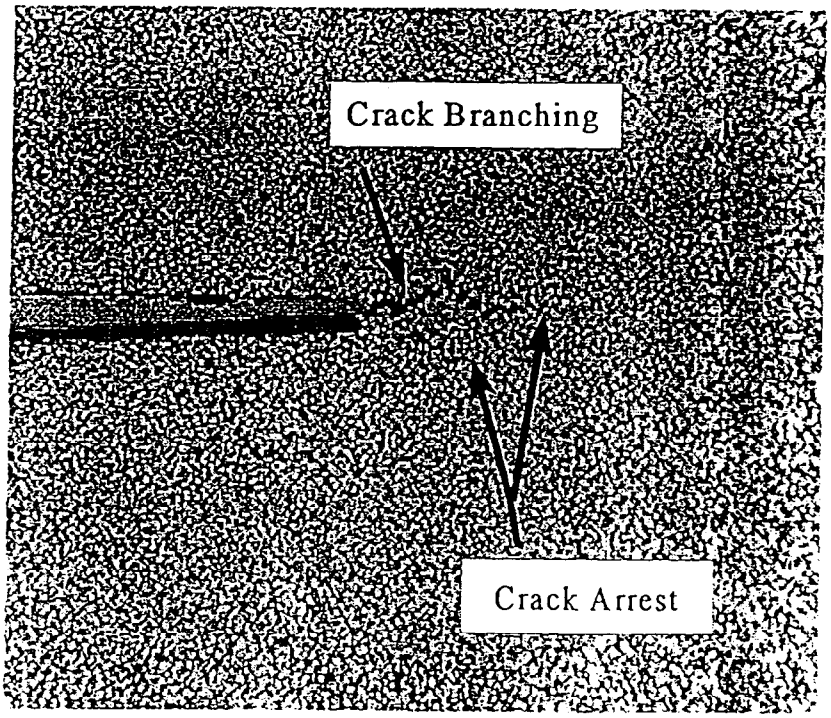

Figure 3.8 Crack Propagation in the 0% RAP Specimen at 22°C.

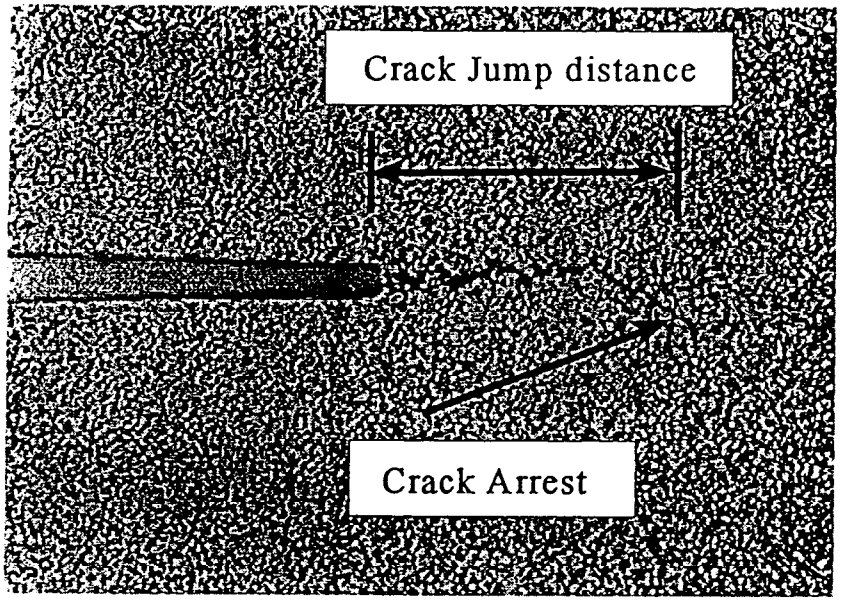

Figure 3.9 Crack Propagation in the 50% RAP Specimen at 22°C.

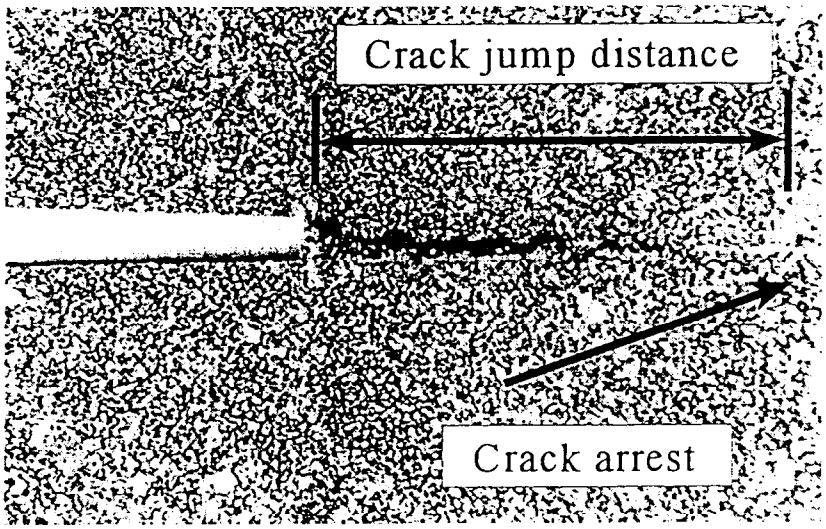

Figure 3.10 Crack Propagation in the 100% RAP Specimen at 22°C.

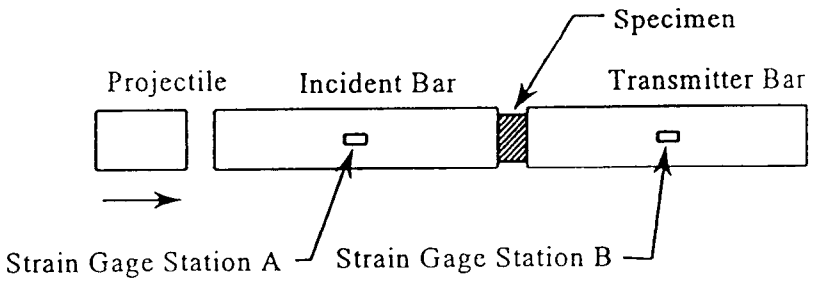

Figure 3.11 Schematic of the SHPB Apparatus.

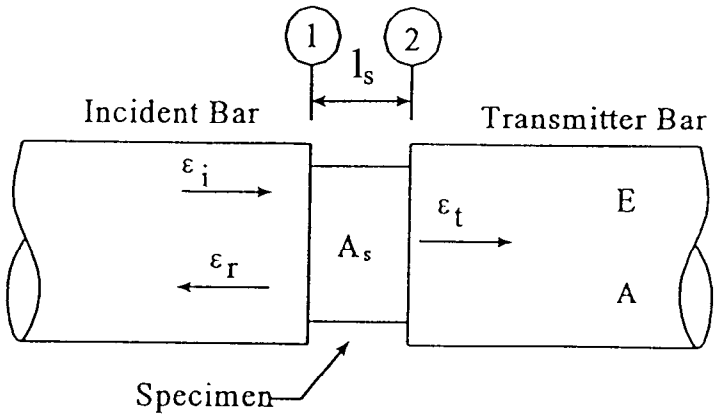

Figure 3.12 Strain Pulses at the Specimen-Bar Interface.

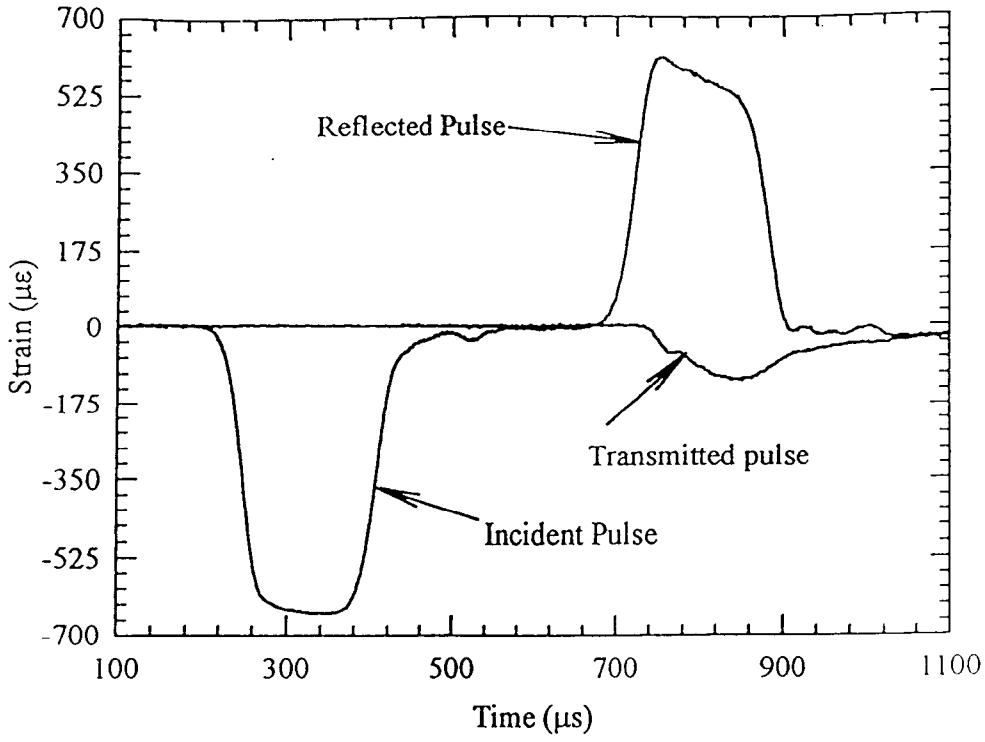

Figure 3.13 Typical Pulses Profiles in the SHPB System.

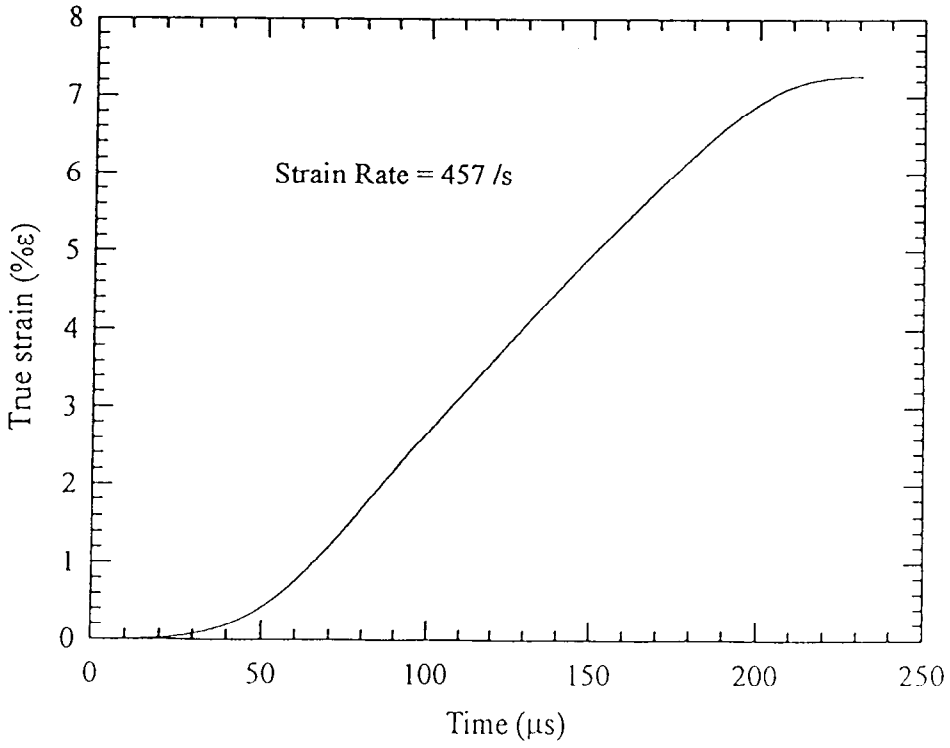

Figure 3.14 Typical Plot of Strain History – Dynamic Loading.

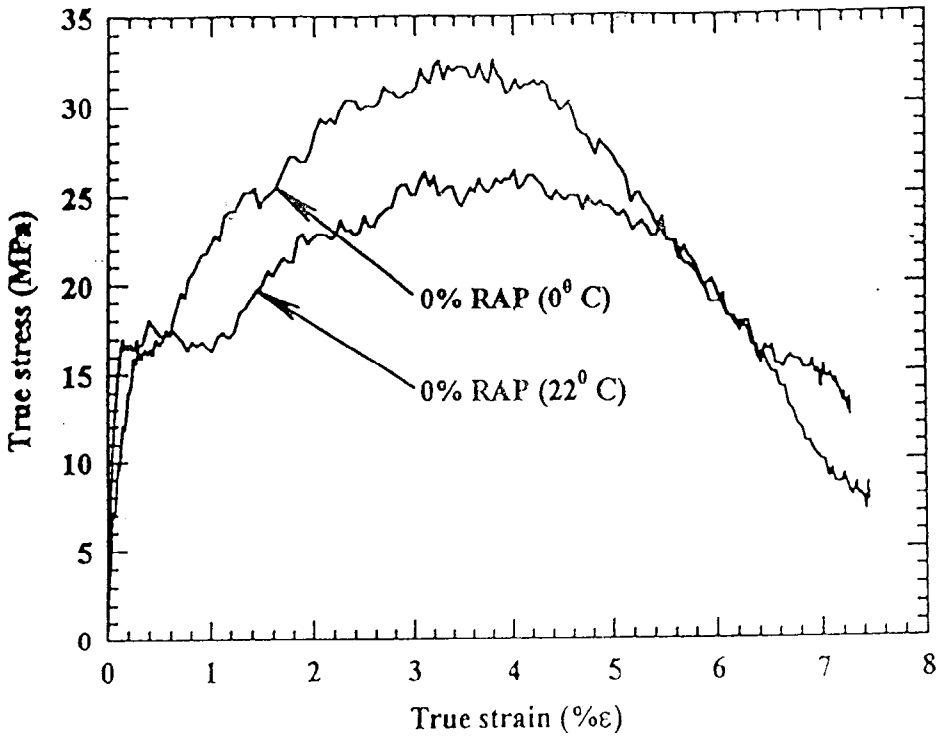

Figure 3.15 Typical Trends in the Dynamic Stress-Strain Response of Base Asphalt Binder at 0 and 22°C.

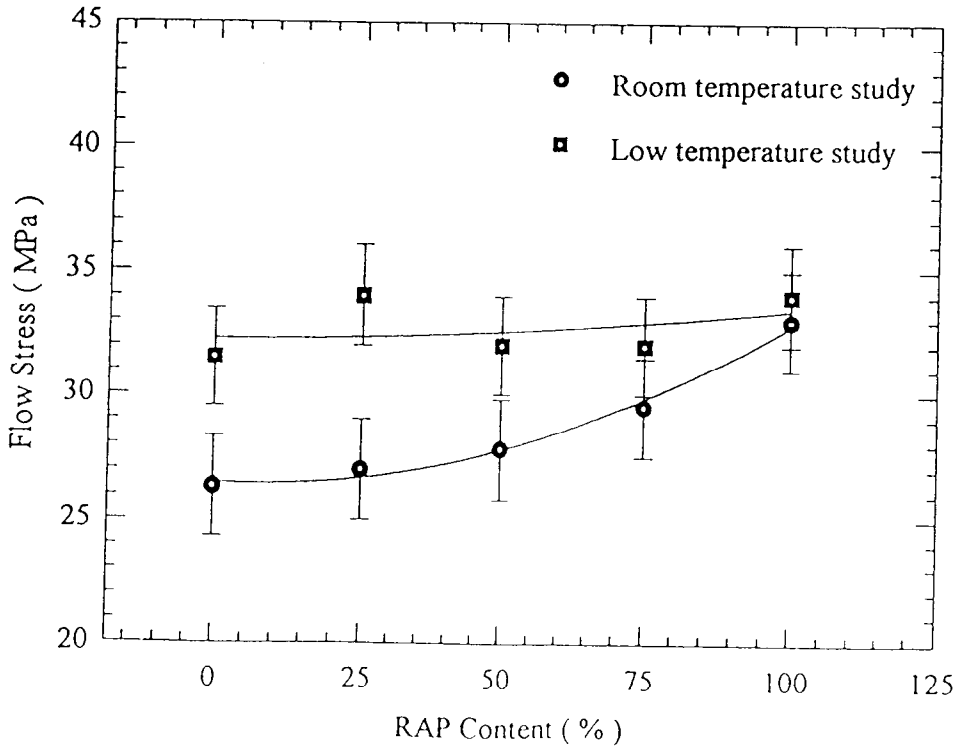

Figure 3.16 Variation of Dynamic Flow Stress with RAP Content.

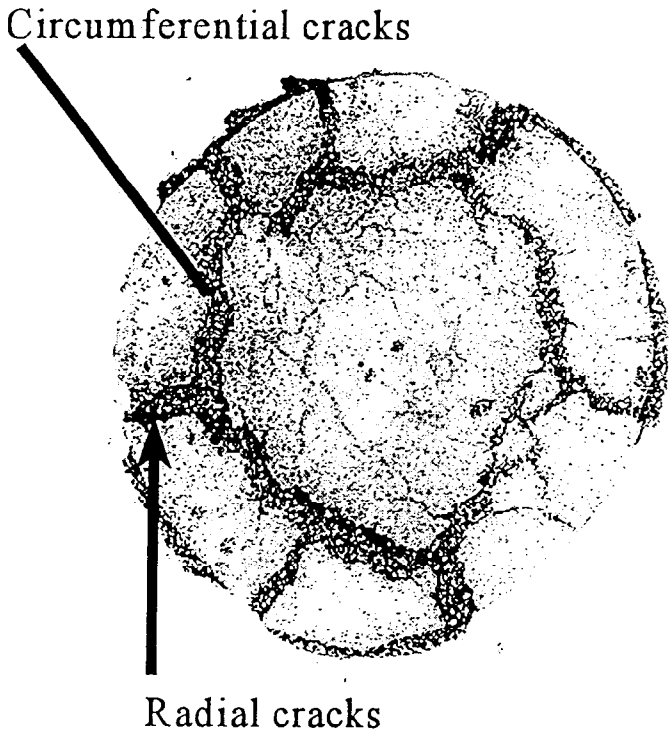

Figure 3.17 Crack Propagation in the 75% RAP Specimen under Dynamic Loading Condition.

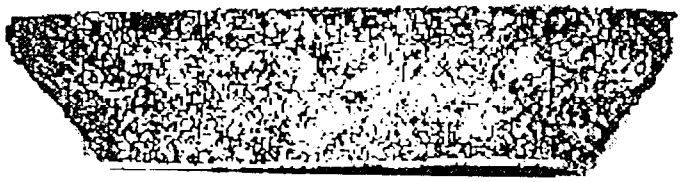

Figure 3.18 Shear Dominance in the 75% RAP Specimen – Typical of all Specimen Tested Dynamically.

4 LOW TEMPERATURE CRACKING

Low temperature cracking is considered as the nonload associated cracking. It is caused by the environmental conditions rather than by applied traffic loads. It is characterized by intermittent transverse cracks that occur at the surface of asphalt pavement. Low temperature cracking forms when HMA pavement subjected to high cooling rates and low temperatures develops tensile stresses due to shrinkage. At some point along the pavement, the tensile stress exceeds the fracture strength of the asphalt concrete and transverse cracking develops. The cracking starts at the surface and progresses down with time.

Since HMA mixes have high stiffness at low temperatures, they are very prone to cracking. Mix stiffness at low temperatures is primarily dependent on the properties of the asphalt binder because low temperatures do not have a significant effect on aggregates in the mix. Therefore, high asphalt binder stiffness at low temperatures is the predominant cause of this type of cracking. In addition, asphalt binder that are excessively aged, because they are unduly prone to oxidation and/or contained in a mixture constructed with too many air voids, are more prone to low temperature cracking.

4.1 Fracture Toughness Test at Low Temperature

The methodology adopted in conducting these set of experiments remained much the same as the previous case except the low testing temperature (0°C). Thus, the cured specimens were soaked in ice for a period of 24 hours, before testing. Three specimens each were tested at every increment of RAP content and an average of the results was reported. The results from the experiments are presented in Figure 3.7. Interestingly, an increase of

30% was noticed in the K_{IC} values from these experiments as compared to that obtained for the 100% RAP specimen at room temperature. The data was fit by a flat trend line, which signifies that the addition of RAP does not have any noticeable effect on the performance of the binder at low temperatures.

A brittle fast fracture occurred in all the specimens tested at this temperature. The crack propagation in the 100% RAP specimen, shown in Figure 4.1 is indicative of this fact. Interestingly, stable crack propagation leading to arrest was observed for the 100% RAP specimen at room temperature, as shown in Figure 3.10. The crack opening displacement was also found lesser at low temperature than what was observed at room temperature.

In the light of visual observations of crack propagation in the specimens at both temperatures, the following can be concluded. The actual numerical values of fracture toughness may be rendered invalid due to the presence of plastic zones at room temperature. This is because fracture toughness is estimated based on the principles of linear elastic fracture mechanics. However, the K_{IC} values obtained at 0°C are definitely valid as the binder behaves as a true brittle material at this temperature. Hence, the increasing trend of K_{IC} with RAP content can be considered to be one leading into brittle behavior, as shown in Figure 4.1. More importantly, it is plausible that there is a ductile to brittle transition in the behavior of the binder as the temperature is varied from room 22°C to 0°C.

4.2 Dynamic Response of Virgin Asphalt and RAP Binders at Low Temperature

Experiments were carried out at low temperature (0°C) in order to determine the low temperature performance of RAP binders under dynamic loading conditions. These sets of experiments were carried out in as much the same way as the room temperature experiments.

The only difference was that the specimens were soaked in an ice bath for a period of 24 hours so as to lower their temperature to 0°C. These set of experiments were also conducted at a nominal strain rate of 450 /s in order to make a comparison of performance. The equipment used and the procedure for acquiring data was much the same as mentioned in the previous section.

The results from these experiments are provided in Table 3.4. There was a marginal increase of 8% in the dynamic flow stress values for the 100% RAP specimen when compared to that of the 0% RAP specimen. The maximum strain (true strain) was also observed to be the same in all the cases. The specimens could not be recovered for postmortem analysis as all of them had fragmented upon impact. This observation is definitely indicative of brittle failure in the specimen.

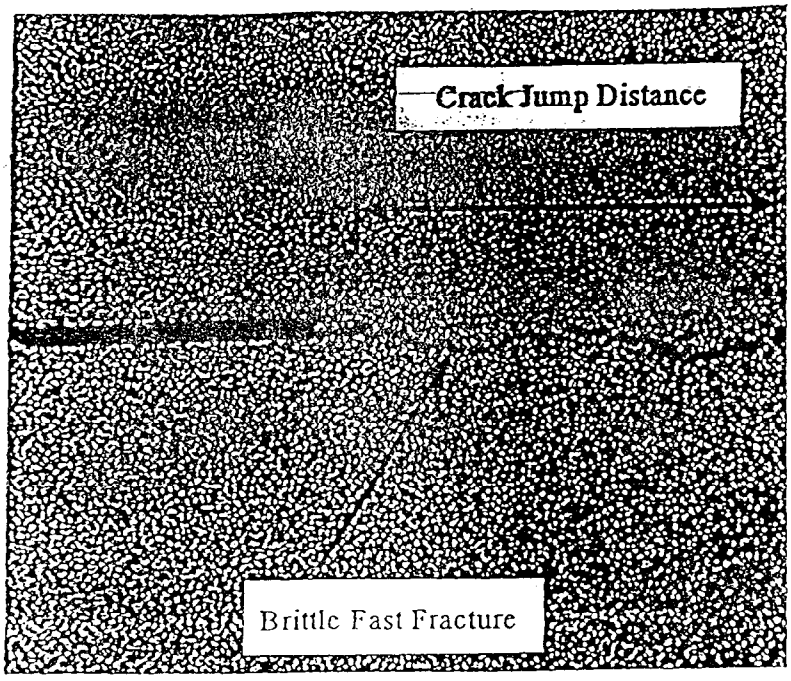

Figure 4.1 Crack Propagation in the 100% RAP Specimen at 0°C.

5 CONCLUSIONS AND RECOMMENDATIONS

The following conclusion and recommendations can be drawn from the present investigation:

1. The viscosity of asphalt binder was increased as the amount of RAP binder increased. The rotational viscosity of 100% L RAP binder was very high, and it did not meet the limit of 3 Pa-s at 135°C.
2. The values of G*/sinδ were increased as the RAP amount was increased. It was also observed that the binder containing Plant L RAP exhibited the higher G*/sinδ and steeper slope than the one containing Plant C RAP.
3. All values of G*/sinδ at 58°C for AC-10 (PG 58-22) base binder met the minimum requirement, i.e., 1.00 and 2.20 kPa for unaged and RTFO aged binders, respectively. It was also true for the AC-20 (PG 64-22) base binder.
4. The values of G*sinδ were increased as the RAP amount was increased, but the increase was due to mainly G*.
5. Linear regression models have been developed between the log-log of the viscosity as well as the log-log of Superpave binder parameters and the amount of RAP in asphalt binders. Relatively high R^2 values indicated that there are a high relationship between two corresponding variables.
6. An increase in RAP binder content causes an increase in dynamic shear. However, the G*sinδ value of PAV aged binder should be less than 5,000 KPa to resist against fatigue cracking.
7. For the quasi-static loading experiments, it was observed that the compressive strength and stiffness were increased as the amount of RAP increased. The increase

in both compressive strength and stiffness reduced the ductility in the specimens as the amount of RAP was increased.

8. The fracture toughness was increased as the amount of RAP increased, at room temperature. However, it was observed that RAP contents had a significant effect on the crack propagation. The crack propagation tended towards instability as the amount of RAP increases, which increased the crack jump distance in the specimen. In other words, RAP binder addition reduced ductility in a specimen.

9. The fracture toughness values of the binder at low temperature were higher than the ones at room temperature. Again, the crack propagation was seen as a brittle fast fracture in a specimen. However, the increase in RAP content did not have any significant effect on the performance of the binder at low temperature.

10. The room temperature dynamic flow stress values of 100% RAP specimen were increased by 25% when compared to the 0% RAP specimen. In the mean time, the dynamic response of the base asphalt binder was not affected by the addition of RAP at low temperature.

11. A comparison of results from the quasi-static and the dynamic experiments indicated an increase in flow stress of many orders of magnitude. Thus, the binder was found to be highly susceptible to rate of loading.

12. It is recommended that further research should be performed at low temperature, e.g. below 0°C to evaluate the low-temperature cracking resistance characteristics of binder with RAP.

REFERENCES

1. *Annual Book of ASTM Standards*. (1996). ASTM E399 "Standard Test Method for Plane-Strain Fracture Toughness of Metallic Materials." Philadelphia, Pa.

2. Brown, R., Kandhal, P., Lee, D. and Lee, K.W. (1996) "Significance of Tests for Highway Materials," ASCE Journal of Materials in Civil Engineering, Vol.8, No.1, pp. 26-40.

3. Davies, E. and Hunter, S. (1963). "The Dynamic Compression Testing of Solids by the Method of Split Hopkinson Pressure Bar," Journal of Mechanics and Physics of Solids, Vol.11, pp 155-179.

4. Jacobs, M., Hopman, P., and Molenaar, A. (1996). "Application of Fracture Mechanics Principles to Analyze Cracking in Asphalt Concrete," Journal of AAPT, pp. 1-39.

5. Kennedy, T., Roberts, F. and Lee, K.W. (1982). "Evaluation of Moisture Susceptibility of Asphalt Mixtures Using the Texas Freeze-Thaw Pedestal Test," Proc. of AAPT. Vol.51.

6. Kolsky, H. (1949). "An Investigation of the Mechanical Properties of Materials at Very High Rates," Philosophical Transactions of the Royal Society of London, Series B, Vol.62, pp 676-700.

7. Lindholm, U. and Yeakley, L. (1968). "High Strain-Rate Testing: Tension and Compression,"Experimental Mechanics, Vol.8, pp 1-9.

8. Majidzadeh, K., Dat, M. and Makdisi-Ilyas, F. (1976). "Application of Fracture Mechanics for Improved Design of Bituminous Concrete," Report No. FHWA-RD-76-92.

9. Malvern, L. and Ross, C. (1985). "Dynamic Response of Concrete Structures," Final Report for the AFOSR Contract No. FR9620-83-K007, U.S. Air Force Office of Scientific Research.

10. May, R. and McGennis, R. (1996) "Superpave Asphalt Mixture Analysis," The Asphalt Institute Research Center, Lexington, KY.

11. McGennis, R., Shuler, S. and Bahia, H. (1994). "Background of SUPERPAVE Asphalt Binder Test Methods," Report No. FHWA-SA-94-069, Washington, D.C.

12. *Mix-Design Methods for Asphalt Concrete and Other Hot Mix Types.* (1993). Asphalt Institute MS-2, 6th ed., Lexington, KY.

13. Monismith, C.L., Hicks, R.G. and Salam, Y.M., (1972) "Basic Properties of Pavement Components," Report FHWA-RD-72-19.

14. Nemat-Nasser, S., Issacs, J. and Starrett, J. (1991). "Hopkinson Techniques for Dynamic Recovery Experiments," Proceedings of the Royal Society of London, Series A, Vol. 435, pp 371-391.

15. *Provisional Standards.* (1996). Am. Assoc. of State Hwy. And Transp. Officials (AASHTO), Washington, D.C.

16. Roberts, F., Kandhal, P., Brown, R., Lee, D., and Kennedy, T. (1991). "Hot Mix Asphalt Materials, Mixture Design, and Construction." NAPA Education Foundation, Lanham, Md.

17. Sousa, J. and Monismith, C. (1988). "Dynamic Properties of Asphalt Concrete," Journal of Testing and Evaluation, Vol.16, No.4.

18. *Standard Specifications for Ttransportation Materials and Methods of Sampling and Testing.* (1993). 16th ed., Part II, AASHTO, Washington, D.C.

19. Sulaiman, F., and Stock, A. (1996). "The Use of Fracture Mechanics for the Evaluation of Asphalt Mixes," Journal of AAPT, Vol. 64. pp 500-533.